VALIDATION OF TRAP DENSITY THEORY IN SINGLE LAYER ORGANIC LIGHT EMITTING DIODES WITH TRIS(8-HYDROXYQUINOLINATO)ALUMINIUM AS THE EMISSIVE MATERIAL

MOHD SUFFIAN BIN ZAINI

FACULTY OF SCIENCE
UNIVERSITI MALAYA
KUALA LUMPUR

2020

VALIDATION OF TRAP DENSITY THEORY IN SINGLE LAYER ORGANIC LIGHT EMITTING DIODES WITH TRIS(8-HYDROXYQUINOLINATO)ALUMINIUM AS THE EMISSIVE MATERIAL

MOHD SUFFIAN BIN ZAINI

DISSERTATION SUBMITTED IN FULFILMENT OF THE REQUIREMENTS FOR THE DEGREE OF MASTER OF SCIENCE

DEPARTMENT OF PHYSICS
FACULTY OF SCIENCE
UNIVERSITI MALAYA
KUALA LUMPUR

2020

UNIVERSITY OF MALAYA

ORIGINAL LITERARY WORK DECLARATION

Name of Candidate: **MOHD SUFFIAN BIN ZAINI**

Matric No: **SGR140010**

Name of Degree: **MASTER OF SCIENCE**

Title of Dissertation ("this Work"):

VALIDATION OF TRAP DENSITY THEORY IN SINGLE LAYER ORGANIC LIGHT EMITTING DIODES WITH TRIS(8-HYDROXYQUINOLINATO) ALUMINIUM AS THE EMISSIVE MATERIAL

Field of Study: EXPERIMENTAL PHYSICS

I do solemnly and sincerely declare that:

(1) I am the sole author/writer of this Work;
(2) This Work is original;
(3) Any use of any work in which copyright exists was done by way of fair dealing and for permitted purposes and any excerpt or extract from, or reference to or reproduction of any copyright work has been disclosed expressly and sufficiently and the title of the Work and its authorship have been acknowledged in this Work;
(4) I do not have any actual knowledge nor do I ought reasonably to know that the making of this work constitutes an infringement of any copyright work;
(5) I hereby assign all and every rights in the copyright to this Work to the University of Malaya ("UM"), who henceforth shall be owner of the copyright in this Work and that any reproduction or use in any form or by any means whatsoever is prohibited without the written consent of UM having been first had and obtained;
(6) I am fully aware that if in the course of making this Work I have infringed any copyright whether intentionally or otherwise, I may be subject to legal action or any other action as may be determined by UM.

Candidate's Signature Date:

Subscribed and solemnly declared before,

Witness's Signature Date:

Name:

Designation:

VALIDATION OF TRAP DENSITY THEORY IN SINGLE LAYER ORGANIC LIGHT EMITTING DIODES WITH TRIS(8-HYDROXYQUINOLINATO)ALUMINIUM AS THE EMISSIVE MATERIAL

ABSTRACT

Organic light-emitting diodes (OLEDs) rapidly evolving as the future of solid-state lighting and display application due to its numerous advantages and features. However, the efficiency, lifetime, and fabrication method still need to be improved. Even in solving efficiency issues in the device, there are many challenges to be addressed and overcome. In theory, charge transport phenomena contribute greatly towards increasing or improving the device efficiency. The magnitude of carrier mobility determines the performance of the device, as it influenced device efficiency. For organic semiconductor such as OLED, space-charge limited current (SCLC) theory was used to determine the mobility of the device. This theory is often true for a very basic structure in a simple organic semiconductor. One of the weaknesses in SCLC theory is that traps phenomena or trap density is neglected and not considered in formulating the mobility of charge carrier. In this thesis, a theoretical model for single-layer OLED that includes trap density is explained with the help of an equation. The focus of this thesis is to analyze and discussed the trap density effect in a single layer OLED. A single layer emissive OLED is fabricated for this project in order to validate the theory presented. Tris(8-hydroxyquinolinato)aluminium (Alq_3) is chosen as the emissive material since it has been researched widely, and much-needed parameters can be easily obtained from previous research. The trap density value obtained at voltage 14 V when OLED A luminesces is 2.40×10^{15} cm^{-3}. It is comparable with other results that have been reported indicating the method used is reliable. The rate of capturing process (trapping), R_n and de-trapping, R_n' of the charge carriers on the localized state of the device are estimated. The parameters R_n and R_n' are plotted on the same graph to observe their relationship with the luminescence of the device. It can be observed that there are two significant regions in

the plot, $R_n > R_n$' and $R_n < R_n$', and the intersection point of R_n with that of R_n' indicate the voltage at which the device luminesces or known as the turn-on voltage of the device. Simulations are then performed by directly increasing the device trap density by two-fold to that of OLED A. The simulation has indicated that trap density has a strong influence on the R_n and R_n' parameters. In order to verify the finding of the simulation, another device (OLED B) with a hole transport layer (HTL) of Poly(N,N'-bis-4 butylphenyl-N,N'-bisphenyl) benzidine (poly-TPD) of 40 nm thickness is fabricated by adding the HTL layer to the existing structure of that of OLED A. It has been proven in this work that OLED B, having a higher value of trap density luminesces at a much lower turn-on voltage, as has been predicted by the simulation results due to the influence of trap density to the parameters of Rn and Rn' of the devices.

Keywords: OLED, Alq_3, trap density.

PENGESAHAN TEORI KETUMPATAN PERANGKAP DI DALAM LAPISAN TUNGGAL DIOD PEMANCAR CAHAYA ORGANIK DENGAN TRIS(8-HYDROXYQUINOLINATO)ALUMINIUM SEBAGAI BAHAN PEMANCAR

ABSTRAK

Diod pemancar cahaya organik (OLEDs) berkembang pesat sebagai peranti untuk kegunaan masa depan pencahayaan fizik keadaan pepejal dan aplikasi paparan kerana mempunyai banyak ciri kegunaan dan kelebihan. Bagaimanapun, kecekapan, tempoh hayat dan proses pembuatan masih perlu dipertingkatkan. Malah, dalam menyelesaikan isu berkaitan kecekapan peranti sahaja pun terdapat pelbagai cabaran untuk ditangani dan diatasi. Secara teori, fenomena pengangkutan cas menyumbang ke arah peningkatkan kecekapan peranti. Magnitud mobiliti pembawa cas menentukan keupayaan prestasi peranti, kerana ia mempengaruhi kecekapan peranti. Dalam semikonduktor organik seperti OLED, teori arus cas-ruang terhad (SCLC) digunapakai untuk menentukan mobiliti peranti. Teori ini biasa digunakan untuk struktur yang sangat asas dalam semikonduktor organik mudah. Salah satu kelemahan dalam teori SCLC ialah, fenomena perangkap atau ketumpatan perangkap telah diabaikan dan tidak dipertimbangkan dalam perumusan mobiliti pembawa cas. Dalam tesis ini, satu model teori untuk lapisan tunggal OLED yang merangkumi ketumpatan perangkap diterangkan dengan bantuan satu persamaan. Fokus tesis adalah untuk menganalisa dan membincangkan kesan kepadatan perangkap dalam lapisan tunggal OLED. Daripada persamaan itu, nilai ketumpatan perangkap untuk satu peranti lapisan boleh ditaksir dan kepentingan nilai-nilai ini dibincangkan secara terperinci. Lapisan tunggal OLED dibina/dibangunkan untuk projek ini bagi mengesahkan teori yang dibentangkan. Tris (8-hydroxyquinolinato)aluminium (Alq_3) dipilih sebagai bahan pemancar kerana ia telah dikaji secara meluas dan parameter yang sangat diperlukan boleh didapati dengan mudah dari kajian yang terdahulu. Nilai perangkap ketumpatan yang didapati pada voltan 14 V apabila peranti OLED A

memancarkan cahaya ialah 2.40 X 10^{15} cm^{-3}. Ianya perbandingan yang selari dengan apa yang telah dilaporkan pihak lain menunjukkan kaedah yang digunakan boleh dipercayai. Kadar pengumpulan(memerangkap), R_n dan kadar melepaskan,R_n' bagi pembawa cas pada ruang setempat bagi peranti dikira. Kedua-dua parameter R_n dan R_n' diplotkan dalam graf yang sama untuk menghubungkaitkan dengan kebolehpancaran cahaya oleh peranti tersebut. Ia boleh diperhatikan terdapat dua rantau yang penting, di mana $R_n > R_n'$ dan $R_n' > R_n$, persimpangan di mana R_n berselisih dengan R_n' menunjukan nilai voltan di mana peranti mula memancarkan cahaya atau voltan penghidup peranti. Simulasi dijalankan dengan meningkatkan nilai ketumpatan perangkap sebanyak dua kali ganda daripada nilai asal OLED A. Simulasi menunjukkan ketumpatan perangkap mempunyai pengaruh yang kuat ke atas parameter R_n dan R_n'. Bagi mengesahkan hasil simulasi, satu lagi peranti (OLED B) dengan lapisan pembawa lohong (HTL) daripada Poly(N,N'-bis-4 butylphenyl-N,N'-bisphenyl) benzidine (poly-TPD) dengan ketebalan 40 nm dihasilkan/dibangunkan ke atas struktur sedia ada OLED A. Telah dibuktikan dalam hasil kerja ini bahawa OLED B, mengandungi nilai ketumpatan perangkap yang lebih tinggi, dengan nilai voltan pengidup peranti yang lebih rendah, seperti yang telah diramalkan oleh simulasi disebabkan oleh pengaruh ketumpatan perangkap ke atas parameter R_n dan R_n' peranti.

Kata kunci: Diod pemancar cahaya, Alq_3, ketumpatan perangkap.

ACKNOWLEDGEMENTS

First and foremost, I would like to praise and show gratitude to Almighty Allah for providing me everything I need in this life. I would also like to express my gratitude and thanks to my supervisor, Prof. Dr. Wan Haliza binti Abd. Majid for giving me the right direction in my research, pointing out all the weakness to overcome, reading materials related to my research until I am able to complete my studies.

I also want to thanks my friend, Mohd. Arif for giving me the opportunity to further studies in the field of physic even though my first degree was in engineering. Thanks for the encouragement in all these years.

A special thanks to Low Dimensional Material Research Center (LDMRC) for providing all the research facilities and resources needed for me to complete my study. The research group "Organic Electronic & ZnO" which I am a part of, is proof that LDMRC already has excellence and well-established research culture.

Most of all, I would like to give thanks MOSTI and UM for the following research grant ER007-2012A, SF019-2013, FP033-2013B, PG107-2015A, RP026B-15AFR, and RP038D-17AFR that has been kindly giving me support financially from start to finish.

And not to forget special thanks to Wong Wah Seng, Nurul Huda, Nurul Izah and Nur Azlin for sharing their knowledge on their respective PhD project, thus inspired and giving me lots of idea for my future PhD research.

Finally, I am very grateful to my family, especially Mak and Ayah, for all their love and support.

TABLE OF CONTENTS

LIST OF FIGURES

LIST OF TABLES

LIST OF SYMBOLS AND ABBREVIATIONS

W_a	:	Anode work function
V	:	Applied voltage
E_g	:	Bandgap energy
Φ_e	:	Barrier height for electron
Φ_h	:	Barrier height for holes
k	:	Boltzmann constant
τ_m	:	Carrier motion time
W_c	:	Cathode work function
T_c	:	Characteristic trap temperature
n_e	:	Charge carrier density of electron
n_n	:	Charge carrier density of holes
μ	:	Charge mobility
N_c	:	Conduction band density of state
E_c	:	Conduction band energy level
J	:	Current density
J_0	:	Current density saturation point
N_{ct}	:	Effective density of states in the conduction band
F	:	Electric Field
μ_e	:	Electron mobility
C_n	:	Electron-capture cross section constant
τ_c	:	Electron-hole capture time
e	:	Elementary charge
E_n	:	Energy in unit constant
τ	:	Excess carrier lifetime

f_F	:	Fermi function
J_{FN}	:	Fowler-Nordheim current density
μ_h	:	Holes mobility
P_t	:	Holes trapping centre concentration
Φ_B	:	Injection barrier
n_i	:	Intrinsic carrier concentration
j_{ohmic}	:	Ohmic drift current
λ	:	Optical photo emission
ε_s	:	Permittivity of sample
T_g	:	Phase transition temperature
π	:	Pi
$\hbar$	:	Plank constant reduced
τ_{rec}	:	Recombination time
ε_r	:	Relative dielectric
m^*_e	:	Relative mass of electron
A^*	:	Richardson constant
J_{RS}	:	Richardson-Schottky current density
E_{tn}	:	Single trap energy level
j_{SCLC}	:	Space charge limited current density
n_0	:	Thermal equilibrium concentration of electron
p_0	:	Thermal equilibrium concentration of holes
$\tilde{v}_e$	:	Thermal velocity of electron
H_t	:	Trap density of states
E_t	:	Trap energy
n_t	:	Trapped electron carrier concentration
p_t	:	Trapped holes carrier concentration

N_t	:	Trapping centre concentration
ε_0	:	Vacuum permeability
N_v	:	Valence band density of state
E_v	:	Valence band energy level
Al	:	Aluminium
Alq_3	:	Tris(8-hydroxyquinolinato)aluminium
AMOLED	:	Active Matrix Organic Light Emitting Diode
Au	:	Gold
CB	:	Conduction Band
EIL	:	Electron Injection Layer
EL	:	Electroluminescence
EML	:	Emissive Layer
EOD	:	Electron Only Device
ETL	:	Electron Transport Layer
F8BT	:	Poly(9,9-dioctylfluorene-alt-benzothiadiazole)
FN	:	Fowler-Nordheim
FPD	:	Flat-Panel Display
HBL	:	Hole Blocking Layer
HIL	:	Hole Injection Layer
HOD	:	Hole Only Device
HOMO	:	Highest Occupied Molecular Orbital
ILC	:	Injection limited current
ITO	:	Indium Tin Oxide
I-V-L	:	Current-voltage-luminescence
LCD	:	Liquid Crystal Display
LUMO	:	Lowest Unoccupied Molecular Orbital

MEH-PPV	:	Poly[2-methoxy-5-(2-ethylhexyloxy)-1,4-phenylenevinylene]
MoO_3	:	Molybdenum trioxide
OC_1C_{10}-PPV	:	2-Methoxy-5-(3',7'-dimethyloctyloxy)-benzene-1,4-diacetonitrile
OLED	:	Organic Light-Emitting Diode
PEDOT:PSS	:	Poly(3,4-ethylenedioxythiophene)-poly(styrenesulfonate)
PET	:	Poly(ethyleneterephthalate)
PL	:	Photoluminescence
PLED	:	Polymer Light Emitting Diode
PMOLED	:	Passive-Matrix Organic Light Emitting Diode
Poly-TPD	:	Poly[N,N'-bis(4-butylphenyl)-N,N'-bisphenylbenzidine]
PPV	:	Polyphenylene Vinylene
PVD	:	Physical Vapor Deposition
RS	:	Richardson-Schottky
SCLC	:	Space Charge Limited Current
SMU	:	Source Measurement Unit
SRH	:	Shockley-Read-Hall
TFL	:	Trap-Filled Limited
TOF	:	Time of Flight
TPD	:	N,N'-Bis(3-methylphenyl)-N,N'-diphenylbenzidine
TSC	:	Thermal Stimulated Current
VB	:	Valence Band
ZnO	:	Zinc Oxide

CHAPTER 1: INTRODUCTION

1.1 Research Background

Climate change is becoming a very popular topic and important issue to discuss due to the fast development of our society, especially in technology advancement and there are approximately 2.7 billion tons greenhouses gases emitted yearly. Currently, there are two typical solutions to the climate change problem. One is reducing the fossil fuel energy consumption by improving energy utilization efficiency, and the other is to generate more energy from long-term renewable energy sources. Organic light-emitting diode (OLED) devices are one of the application examples that are utilizing energy efficiency and thus reducing the amount of carbon dioxide released yearly. OLED devices consists almost 90% of glasses and therefore easily be recycled at the end of their operating life.

1.1.1 History of Organic Light-Emitting Diode

Organic electroluminescence research became popular around 1970s and 1980s when researchers found that conductivity of certain organic materials could be changed over the full range from insulator to conductor by chemical doping. In 1963, Pope et al. (1963) reported the first electroluminescence (EL) originated from an organic molecule, anthracene. The achievement did not stimulate much research interest due to the non-practicality, extremely high applied bias voltage around 100 V. Bridge and Vincent (1972) achieved bright blue EL from the vacuum-deposited anthracene crystal film of 0.6 μm thickness with improved applied bias voltage of less than 100 V.

Shirakawa et al. (1977) successfully synthesis the first polymer, polyacetylene, which was capable of conducting electricity. Subsequently MacInnes et al. (1981), showed polyacetylene with oxidative doping can increase conductivity by twelves magnitude. The breakthrough came from Tang and VanSlyke (1987), whose work consisted of a working device with a layer of aromatic diamine (TPD) and a layer of Tris(8-

hydroxyquinolinato)aluminium (Alq_3), the latter being a luminesce layer, with brightness and exceptionally high external quantum efficiency which was achieved at an applied bias voltage below 10 V.

Following this, Adachi et al. (1989) successfully fabricated a stable multilayer device with holes and electrons transport layers between the two electrodes. Tang and VanSlyke (1989) developed a laser-dye doped Alq_3 multilayer structure, which featured a variety of colour emission from original green to the dopant emission colour with improved fluorescent efficiency.

The first polymer light-emitting diode (PLEDs) was discovered by Burroughes et al. (1990) with a precursor polymer of luminescent poly-(phenylene vinylene)(PPV) spin-coated onto an indium tin oxide (ITO) coated glass. Fluorescent emission of singlet exciton is the main mechanism of light emission. To overcome the theoretical limit, which the ratio of forming spin-singlet states and spin triplets is 1:3, Baldo et al. (1998) dope a fluorescent host layer with phosphorescent molecules. The phosphorescent OLEDs demonstrated EL that is due to triplet emission.

In 1992, a fully flexible polymer LED on poly(ethyleneterephthalate)(PET) substrates were fabricated by Gustafsson et al. (1992). Polyaniline anode were used in their devices to overcome the brittle properties of indium tin oxide. Gu et al. (1997) demonstrated a vacuum-deposited OLEDs on ITO-coated polyester substrates. In their report, the flexible OLEDs did not deteriorate after repeated bending.

The first commercial product was an OLED display for automotive application produced by Pioneer Corp. in 1997. Sony Corp. introduced the first OLED TV called XEL-1 ten years later, in October 2007 with a thickness merely 3 mm. The following year, the first OLED lamp was announced by OSRAM with 10 OLED panels, each with

132 x 33 mm in size. Samsung, in 2011, announced a smartphone which first featured a transparent active-matrix organic light-emitting diode (AMOLED) display.

1.1.2 Achievement for OLED

The first low-voltage OLED was developed by Kodak using a simple bilayer structure. Kanno et al. (2006) introduced phosphorescent emitters through efficient intersystem crossing which harvest both singlet and triplet excitons activated by the presence of a heavy metal element in the emitter and thus increased the device efficiency by quadruple. By mixing different coloured emitters, Lee et al. (2008) demonstrated the first white OLED.

After that, Xu et al. (2009) fabricated an improved OLED, by combining a substrate that has a high refractive index with a sophisticated emitter layer using a periodic out-coupling structure that the efficiency is on par with white fluorescent tube. The device reportedly achieved a power efficiency of 1000 cd/m^2 at 90 lm/W. Features such as high colour quality and substrates over a large area, OLED can potentially replace fluorescent lights with reduced energy costs. Organic electroluminescent devices has full-colour capability which is a must requirement for flat-panel display application and practical uses.

Modification of patterned substrates by using high-refractive-index glass was used to solve the mismatch between substrate and its organic materials, resulting in higher efficiencies up to 90 lm/W. OLEDs can provide revolutionary lighting properties, such as excellent transparency, colour tunability, and flexible lighting sources. The flexibility allows OLEDs to operate effectively when designed for spaces with certain constraint such as small-sized apartment, offices and even in transportation such as bike and cars.

OLEDs potential are driven by different manufacturing processes, holds many advantages over its predecessor, the flat-panel displays. In term of cost in for large-area displays, OLEDs easily surpasses liquid crystal display (LCD) by using inkjet technology

which the substrate can be printed on. Even in bright light, OLEDs screen able to provide a distinct and clear image, and viewing angle up to 160°. Unlike LCDs, OLEDs do not have backlights (added bulk and weight). Characteristic such as Lambertian self-emission, high luminous efficiency, fast response time, low operation voltage, lightweight, robustness to external impact make OLED devices ideal for flat-panel display (FPD) application.

OLEDs technology advancement started with a simple target just for displays and small screen application. In 1999, the passive-matrix organic light-emitting diode (PMOLED) started shipments while the AMOLED started near the end of 2002. OLED display revenue expected to grow about $44 billion in 2019 from total product revenue, compared to just $4 billion in 2011 and $826 million in 2009. The main display for mobile phone will continue to lead in revenue for the next several years.

1.2 Research Problem and Motivation

Since the start of successful fabrication of OLED by Tang and Vanslyke, the researcher suggested the use of electrical and optical modelling to provide direction and detailed understanding of the physical processes governing the macroscopic device behaviour and to enable rapid exploration of possible device parameter space. This gives birth to theoretical models such as Space Charge Limited Current (SCLC) (Rose, 1955), Trap Filled Limited (TFL) (Haering & Adams, 1960), Richardson-Schottky (RS) (Simmons, 1965) and Fowler-Nordheim (FN) (Lenzlinger & Snow, 1969). Nevertheless, all of these models have several restrictions and require further simplifications in order tp estimate certain values or parameters.

A good example of this would be the SCLC injection model. One of the simplifications/restrictions is that the trapping phenomena are completely ignored/neglected. Research has shown that trap density is crucial in organic

semiconductor since all organic materials contain impurity and trap density affect the performance of the device. A common misconception in organic materials study is that trap density is caused only by the chemical impurities during synthesis. Shockley-Read Hall (SRH) theory (Hall, 1952; Schenk, 1992; Shockley & Read Jr, 1952) take into consideration of the trap density definitions and their importance during the carrier's recombination process. It becomes clear that knowing more about trap density would lead to a better understanding of electrical properties in OLEDs.

1.3 Research Objectives

The objectives of this research are as follow:

i To describe and accurately show that trap density in OLEDs are not just impurities or defect, but importantly, act as center for the recombination process for the electron and hole charge carriers.

ii To propose a simple and reliable method to estimate the trap density of an OLED device from the current-voltage characteristic measurement.

iii To propose a technique that manipulates trap density to analyze a single layer OLED device and optimized its current-voltage-luminescence characteristic based on a theoretical simulation approach.

1.4 Scope of Research

OLED devices fabricated in this work consist of only up to two layers of organic materials (the emissive and hole layer transport). The current-voltage characteristic presented in the theoretical part remain valid and follows the SCLC model. Multiple layers of organic material or a much more complex structure would suggest a much more complicated current-voltage modelling such as Monte-Carlo (MC) approach instead. The emissive material in this work, Alq_3 is a well-known single-molecule and well-studied.

Thus, the parameters needed to evaluate all the calculation are readily available. A different type of emissive material such as Poly[2-methoxy-5-(2-ethylhexyloxy)-1,4-phenylenevinylene] (MEH-PPV) is still extensively being studied, but the parameters required is not available. The characterization technique used in this research only involved the current-voltage-luminescence and topic as such quantum efficiency, carriers mobilities, device morphology, lifetime study is beyond the scope of this thesis.

1.5 Thesis Outline

Chapter 2 presents the literature review on OLEDs devices and principle theories in such devices. Topics such as atomic orbital, chemical bands, and their energy levels will be discussed thoroughly. The basic principle of OLEDs operation such as charge injection, charge transport, recombination, and light emission will be covered. Chapter 3 explains in details the method used to complete the theoretical study. Shockley-Read-Hall Theory and Nanocrystalline Semiconductor Theory are used to define and describe the trap density. Chapter 4 focuses on the details of device fabrication and characterization technique used for this work. From the substrate to solvent preparation, thin-film formation, and physical vapor deposition (PVD), and lastly the characterization technique involved to complement the theoretical studies. Chapter 5 discusses the trap density effect on single-carrier devices. Trap density calculation from the current-voltage characteristic is also shown and the results are compared with the values obtained by others. Chapter 6 provides the results on single layer OLED with two types of carriers. Details of trap density effect on the current-voltage-luminescence (I-V-L) are also included. Chapter 7 gives a summary and suggestion for further work related to the study of trap density. The summary of the research flow of this dissertation is shown in Figure 1.1.

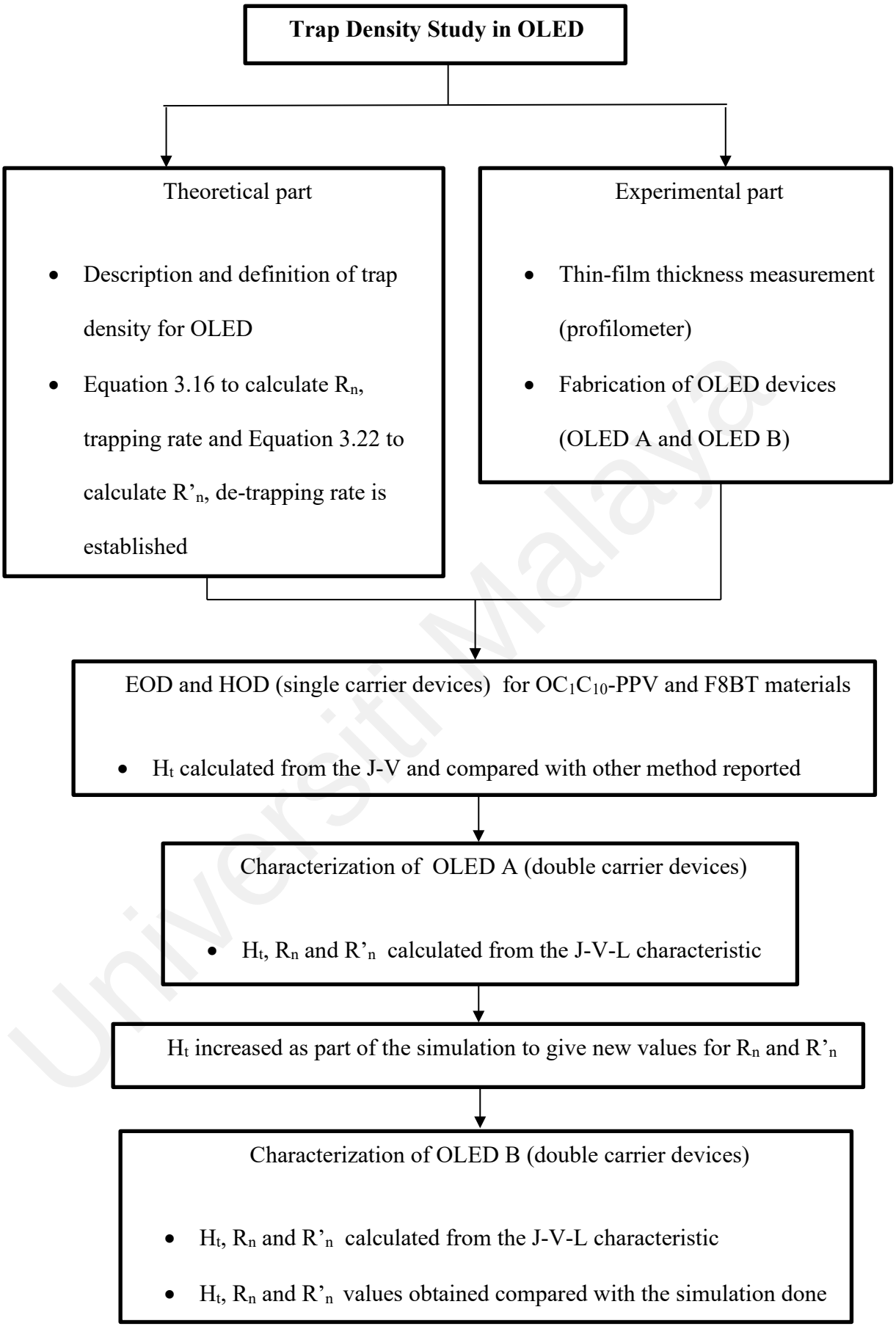

Figure 1.1: Research work design and summary.

CHAPTER 2: LITERATURE REVIEW

2.1 Introduction

This chapter presents a literature review on organic semiconductor theory and the fundamental properties of conducting organics in OLEDs. The description of how organic molecules or materials conduct electricity, absorption, and emission phenomena are provided. The main focus will also be on the band energy theory, details on the structure and the construction of the devices, including how OLED devices work. Basic characterization consists of optical and photoluminescence, electroluminescence and impedance studies will be discussed as well.

2.2 Organic Semiconductors

For the case of inorganic semiconductor, the structure heavily depends on the ionic or strong covalent bonding between atoms in the lattice point. These bonds create strong interactions between atomic orbital inside the structure. What differs in organic semiconductor would be the much weaker interaction among the atoms/molecules. Since the molecular orbital overlapping is small, the molecular bonding is weaker compared to inorganic materials. organic semiconductor compound are consist of conjugated bonding structure. These conjugated bond structure can be seen in either small molecule or polymer materials. Conjugated bonds are built from an alternation between single and double chemical bonds in the structure. A polymer is defined as an organic compound that contains repeating monomer meanwhile compound that does not have repeating monomer structure is called small molecule. Small molecule materials do not have repeating monomers structure, which makes them smaller in size compared to polymer, and they are also known as macromolecules. Examples of small molecule and polymer compound that are well-known in organic electronics are shown in Figure 2.1 and Figure 2.2, respectively. Alq_3 small-molecule OLED devices have been used extensively by

researchers to investigate the theoretical analysis specifically on the electroluminescence mechanism and optical properties of organic semiconductor devices.

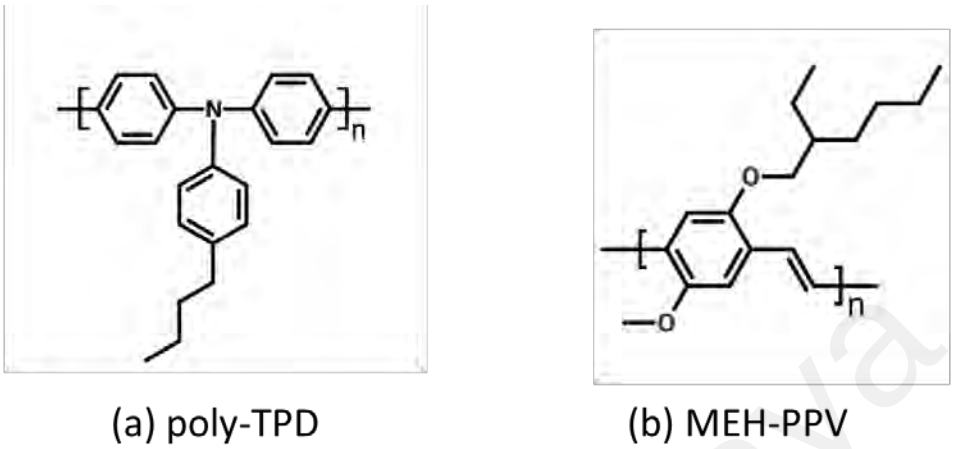

Figure 2.1: Molecular structure of polymer materials (a)poly-TPD and (b) MEH-PPV that is commonly used in OLED devices.

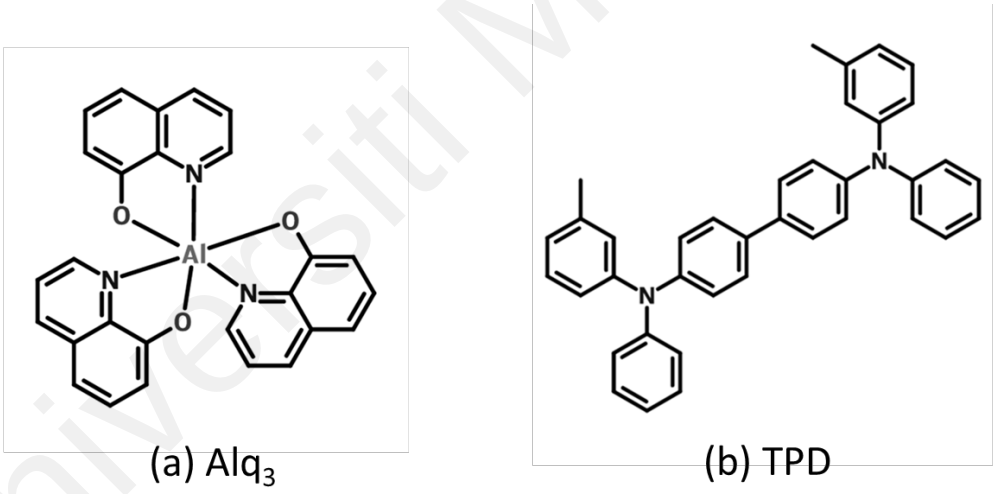

Figure 2.2: Molecular structure of small molecule materials (a)Alq_3 and (b) TPD which is widely used in OLED devices.

Conjugated structure controls the molecular energy level for the organic compound. A classic example is benzene ring, as shown in Figure 2.3. In benzene structure, the carbon atom has trigonal Sp^2 hybrid orbital which forms the σ-bond and π-bond. In σ-bond, the electrons are strongly localized, and they are known as σ electron. Localized simply means that the σ electron needed very high thermal energy to be removed from its orbital

energy. Meanwhile, π-bond is created from the overlapping of $2p_z$ orbital. Similarly, the occupying electrons in π-bond would be called π electrons. These π electrons inside the conjugated structure are weakly bonded over the carbon atoms and delocalized. Delocalized defined as electrons that can easily move between neighbouring atoms, and the compound exhibits semiconductor properties. Large conjugated structure enables a broad range of delocalized π electrons, meaning more electrons are capable to hop from one atom to another.

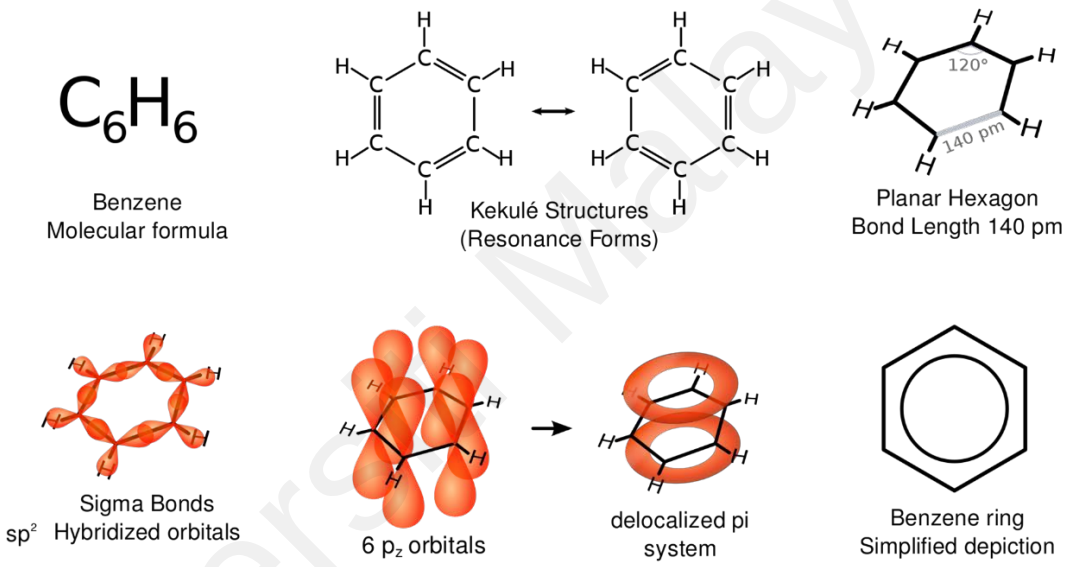

Figure 2.3: Molecular structure of benzene and its orbital system. (Wikipedia, 2019)

The π electron is the most significant feature in the electrical and optical properties of organic semiconductor when delocalized. Due to its electron spin, the π molecular orbital will be split into two separate energy level. The molecular orbital, which is occupied and having energy levels lower compared to the atomic orbital, are called bonding molecular orbital (π orbital). The π orbital makes the highest occupied molecular orbital (HOMO) and defined as a distribution of energy band of the electron in the molecules. The other molecular orbital is unoccupied and has large energy levels compared to the atomic

orbital, and commonly known as anti-bonding molecular orbital (π^* orbital) and known as the lowest unoccupied molecular orbital (LUMO), defined as the easiest path for the electron excitation from the lower levels. HOMO and LUMO identified as the analogues valence band (VB) and conduction band (CB) in metal or inorganic semiconductor. The difference between these energy levels represent the bandgap of the compound, and it depends on the configuration and size of the conjugated structure.

2.2.1 Organic Materials as an Emissive Layer

The most basic concepts of organic semiconductor, including the electrical and luminescence part, are based on inorganic semiconductor physics. But one should note their differences and specialties. Example of organic materials used as emissive layer are Poly[3-(carbazol-9-ylmethyl)-3-methyloxetane](Jou et al., 2011), Poly[9-sec-butyl-2,7-difluoro-9H -carbazole](Mizuno et al., 2012), and poly(9,9-dioctylfluoreneco-bithiophene)(Xu et al., 2012). Most small molecules and polymeric materials used in OLEDs device usually form disordered amorphous thin films without macroscopic crystal lattice, both low molecular weight and high molecular weight. This is the main reason for the difficulty of applying principles developed for inorganic molecule crystal. Another reason would be the fact that charges are transported randomly by hopping between localized states due to the absence of extended delocalized states. The charge carrier transport with stochastic behaviour contribute to low mobility (less than one cm^2/Vs). For organic materials, impurities act as a source of extrinsic mobile charge carrier, and also contributes to charge carriers trap. More details and discussion of traps in organic semiconductor are discussed in the next chapter (Chapter 3).

2.2.2 Band Energy Theory

The electrical and optical properties of solid materials are determined dominantly by their structures on the energy band diagram. These electronic energy band diagrams can

be categorized as insulator, semiconductor, and metals. In the energy band diagram, two distinct energy bands in which electrons exist, are called conduction band (CB) and valence band (VB). These two bands are separated by an energy gap, which is defined as the forbidden gap. Figure 2.4 shows the energy band diagrams for insulator, semiconductor, and conductor. The main characteristic of metal (i.e. conductor) includes a very low resistivity, the conduction band is either partially filled (which many electrons are available) or overlaps the valence band so that there is no forbidden gap at all (Bell ,1980; Neaman, 1992; Sze, 2008). An insulator is characterized by a large forbidden gap, and the energy band for an insulator is either completely empty or full. The resistivity value would be very large, and the conductivity becomes too small; hence no charged particle can contribute to drift current. Bandgap energy, E_g for insulator, is very large, in the range > 6 eV (Sze, 2008). An inorganic semiconductor has much smaller bandgap, E_g, around 1 eV. Organic semiconductor materials mostly have a large energy gap between 2-3 eV (Neaman, 1992).

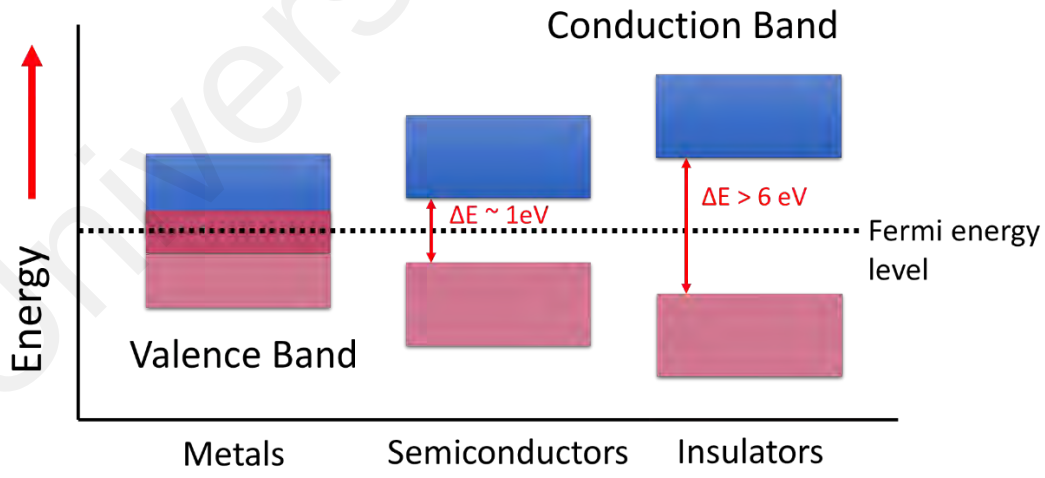

Figure 2.4: Energy band diagram for insulators, semiconductors, and metals.

2.3 OLED

It is very crucial to know and understand how the OLED structure works and the roles for each layer of the device used. The fundamental and details of how OLED devices work theoretically will be discussed thoroughly in this section:

2.3.1 OLED Structure

Figure 2.5 shows the basic structure for OLED devices. A transparent anode material is needed (i.e., Indium-Tin-Oxide(ITO)) stacked on top of a glass substrate. An emissive layer, organic materials such as Tris(8-hydroxyquinolinato)aluminium(Alq_3) sandwiched between the anode and cathode which the cathode is usually a thermally deposited metal (i.e., Aluminium(Al)). The emission of light will occur at the emissive layer, progressing towards the glass substrate. It is very important to understand the theoretical concept behind OLED.

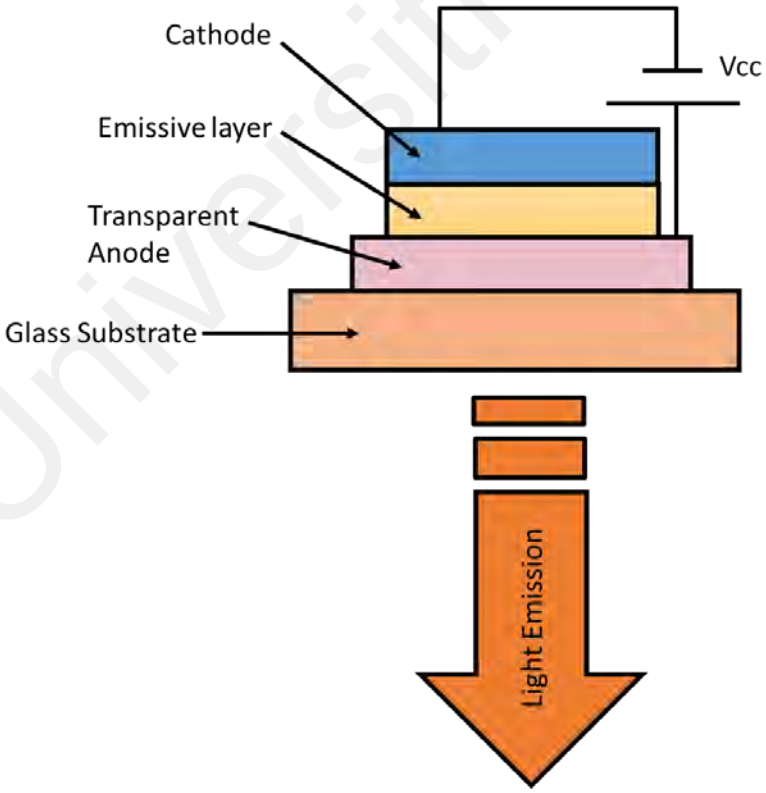

Figure 2.5: Basic structure for OLED devices.

2.3.2 Theoretical Concept of OLED

In theory, the principle operation of OLED devices can be explained and divided into four processes, namely charge carrier's injection, charge carrier transport, charge carrier recombination, and light emission.

2.3.2.1 Charge Carrier Injection Mechanism

An OLED device electroluminescence systematically occurs through combinations of multiple mechanisms and processes. The first and most important mechanism is charge carrier injection from a metal electrode into the organic semiconductor materials.

In contrast to inorganic devices, the current-voltage characteristics of OLED always shows a non-linear behaviour due to their disordered nature (Shuttle et al., 2010). The charge injection process is described as the mechanism of charge carriers passing through a surface boundary or interface contact. The total amount of charge carrier travels through mostly depends on the applied electric field and charge injection barriers at the metal-organic contact. The injection barrier for the electron is $\Phi_e=W_c-A$, and for holes by $\Phi_h=I-W_a$, where W_c and W_a are the work functions of cathode and anode materials. The symbol A and I are the electron affinity and ionization potential of the materials. For organic materials, I and A are referred to the HOMO and LUMO energy levels. The current density J can be denoted by a general equation of Shockley diode (Sah, 1991):

$$J = J_o\left(\exp\left[\frac{qV}{nk_BT}\right]-1\right) \tag{2.1}$$

where J_0 is the current density at saturation point, V is the applied voltage, q is the elementary charge, k_B is the Boltzmann constant, n is the ideality factor, and T is the temperature. If the charge carrier injection from the metal electrode into the organic semiconductor layer occurred via thermionic emission, it is usually referred to as

Richardson-Schottky (RS) (Lye & Dekker, 1957) and Fowler-Nordheim (FN) model (Lenzlinger & Snow, 1969) used for charge carrier injection through tunneling. For the case of thermionic emission, the current density, J_{RS} with an injection barrier, Φ_B is given by (Bhuiyan et al., 1988):

$$J_{RS} = A^* T^2 \exp\left(-\frac{\Phi_B}{kT}\right) \tag{2.2}$$

with

$$A^* = \frac{4\pi q m^* k^2}{h^3} \tag{2.3}$$

where, A^* is the Richardson constant, and A^* = (120A/(cm^{2}K^2) for $m^*=m_0$, and Φ_B is defined as the injection barrier. For the case of FN modelling, it ignores the Columbic effects and only considers the charge tunnelling, where the current density, J_{FN} can be denoted as (Fowler & Nordheim, 1928):

$$J_{FN} = \frac{A^* q^2 F^2}{\Phi_B \alpha^2 k^2} \exp\left(-\frac{2\alpha \Phi_B^{3/2}}{3qF}\right) \tag{2.4}$$

with

$$\alpha = \frac{4\pi\sqrt{2m^*}}{h} \tag{2.5}$$

The FN tunnelling injection of carriers can also be simplified into (Kevin, 2003)

$$J_{FN} \propto F^2 \exp\left(\frac{-K}{F}\right) \tag{2.6}$$

with

$$K = \frac{8\pi\left(2m^*\right)^{1/2}\phi^{3/2}}{3qh} \tag{2.7}$$

where we can write into

$$\ln\left(\frac{J_{FN}}{F^2}\right) \propto -K\frac{1}{F} \tag{2.8}$$

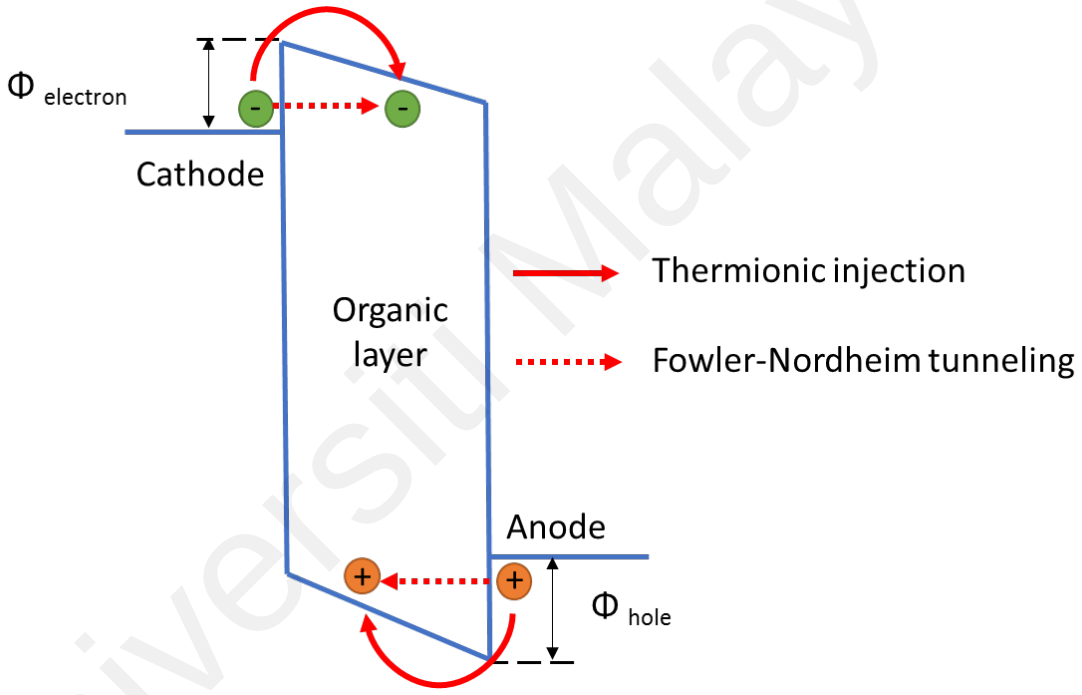

Figure 2.6: Schematic diagram showing the comparison between thermionic emission and Fowler-Nordheim tunneling mechanism.

Figure 2.6 shows the diagram of both thermionic and FN injection mechanisms. Φ_{hole} and $\Phi_{electron}$ are the barrier height for hole and electron injection. These two models are compatible with inorganic semiconductors with boundaries and conditions such as having a larger mean free path and extended band state. However, these models cannot be used in organic semiconductors and become invalid due to the nature of organic materials,

having a very small average mean free path. Furthermore, the presence of disorder atoms or molecule in organic semiconductors can create intermolecular resistance contributing to variable energy barriers that the injected carriers have to overcome. In the end, most of the injected carriers fall back into the metal electrode (Crone et al., 1999). An appropriate model for organic diodes has been suggested by (Davids et al., 1997). The model is presented with assumption that the energy barrier for electrons injection is much larger than for holes ($\Phi_{electron} > \Phi_{hole}$), making the current flow in the devices dominated by holes. Since current flow is dominated by holes, the total current is the sum of three particle components, thermionic emission, interface recombination current and tunneling. Total current, J_p is given by the following equation

$$J_p = -J_{th} + J_{ir} - J_{tu} \tag{2.9}$$

where

J_{th} = thermionic emission current

J_{ir} = interface recombination current

J_{tu} = tunneling current

From Equation (2.9), this model defined the thermionic emission current as the RS in Equation (2.2), thus $J_{th} = J_{RS}$. The interface recombination current is proportional to hole density at the interface which gives

$$J_{ir} = \frac{AT^2}{n_0} n_p \tag{2.10}$$

n_0 is defined as hole density at metal conductor interface and n_p as hole density at organic materials interface. The tunneling current is calculated using the Wentzel–

Kramers–Brillouin (Habault, 1999) approximation through a potential and is given by the following equation

$$J_{tu} = J_t \left(\frac{E_i}{E_t} \right)^2 \exp\left[-\frac{E_t}{E_i} \right] \tag{2.11}$$

where

$$J_t = \frac{e\Phi^2}{9(\pi a_0)^2 \hbar R} \tag{2.12}$$

and

$$E_t = \frac{4\Phi^{\frac{3}{2}}}{3ea_0\sqrt{R}} \tag{2.13}$$

E_i is defined as the energy level at the interface of metal-organic and E_t is the trap energy at the interface, while R is the Rydberg constant and a_0 is the Bohr radius. This unified device model suggest that the charge injection is highly dependent on the voltage bias used. At smaller bias, J_{RS} becomes the dominant injection mechanism which we can simplified Equation (2.9) as

$$J_p \approx J_{RS} \tag{2.14}$$

and when the bias voltage is large, the charge injection is dominated by the tunneling instead which Equation (2.9) becomes

$$J_p \approx J_{tu} \tag{2.15}$$

The bias voltage which tunneling exceeds the thermionic emission depends on the size of the energy barrier height.

2.3.2.2 Charge Carrier Transport Mechanism

The charge carriers are transported into the organic material and would eventually reach the opposite electrode and follow the applied field direction. The transportation process of the charge carriers inside the organic semiconductor is the net total of charge carrier diffusion and hopping processes. Charge carrier diffusion would occurred due to the thermal energy which the diffusion process attempting to make the carrier density uniform, moving from the region where the density is high to the region where the density is low. Hopping mechanism is a result of charge carrier movement among neighbouring molecules. The flow of injected carriers within the organic materials are strongly dependent and is limited by the injection barrier. For a typical organic LED device parameter, when the energy barriers is less than 0.3-0.4 eV, the current obey the space-charge, and the electric field in the structure is highly nonuniformed. For larger energy barriers, injection limited described the current flows and the electric field becomes nearly uniform and the space charge effects can be neglected.

In an organic semiconductor, the charge transport increased when a very low electric field applied in the system and the current obeying the Ohmic drift current:

$$j_{ohmic} = n_o q \mu \frac{V}{d} \tag{2.16}$$

where n_0 is the charge carrier density, q is the electrical charge, μ is the charge carrier mobility, V is the measured applied voltage and d is the thickness of the device. However, for the case of an organic semiconductor which has very low free-carriers density and

very low mobility of charge carriers, it becomes nearly impossible to transport more injected carriers even when applying very high voltage to the device. Eventually, the trapped carriers would create an internal field that is impeding more charge carriers from being injected and thus limiting the current flowing inside the device. Based on the charge injection efficiency and charge carriers mobility, the current will either follow the space-charge limited current (SCLC) (Donovan & Wilson, 1981) or injection limited current (ILC).

One of the critical characteristics of SCLC is that it would require one of the metal-organic contacts is sufficient enough to trap more charge carrier. Eventually, the charge carriers mobility becomes low and independent from the electric field; thus, the organic material becomes an insulator instead of a semiconductor. Using an assumption that the material is without an intrinsic carrier and becomes a perfect insulator, the SCLC model is explained by Mott-Gurney equation (Lampert & Mark, 1970; Weiser, 1970):

$$j_{SCLC} = \frac{9}{8}\varepsilon_r \varepsilon_o \mu \frac{V^2}{d^3} \tag{2.17}$$

where ε_o is the permittivity constant, and ε is the dielectric constant. This equation is used for a trap-free SCLC with a specific condition where the diffusion and the boundary condition at injecting contact are ignored. A trap-free SCLC has a very high carrier density at the metal-organic contact and becomes close to infinity. Injection-limited current (ILC) phenomena only happened when the injection barrier is extremely large, resulting in insufficient carrier injection from the metal electrode into the organic materials. For the case of ILC, the charge carriers would require very high voltage applied to overcome the injection barrier.

2.3.2.3 Charge Carrier Recombination Mechanism

In the electroluminescence process, the recombination of electron and hole is very important since it would create the formation of an exciton (a pair of hole and electron) or the radiative photon energy decay. Recombination mechanism happened if an element with thermal energy, kT moved and trapped within the Columbic potential of the other element. The other element remained idle and static at a distance much less then Columbic distance, r_c from each other. The coulomb attractive potential energy would become equal to the thermal energy at this certain distance and given by:

$$\frac{e^2}{4\pi\varepsilon_o\varepsilon_r r_c} = k_B T \tag{2.18}$$

The term r_c is defined as the thermal capture radius and given by the following expression

$$r_c = \frac{e^2}{4\pi\varepsilon_o\varepsilon_r k_B T} \tag{2.19}$$

The process of carrier recombination in classical physics is related to two mechanism as described by, Langevin (1903) and Thomson (1924). The recombination process related to OLED devices would follow the Langevin type. The expression for the recombination rate as describes by Langevin is:

$$R_{Lan} = \frac{e(\mu_e + \mu_h)}{\varepsilon_o\varepsilon_r} n_e n_h \tag{2.20}$$

where n_e and n_h are the charge carrier densities of electron and holes respectively, ε_o is vacuum permeability, and ε_r is the relative dielectric constant, μ_e and μ_h are the electrons and holes mobilities. The Langevin mechanism can also be related with time relative

parameter. The recombination time, τ_{rec} is defined as a combination of the carrier motion time, τ_m and the electron-hole capture time, τ_c and is given by the following equation:

$$\tau_{rec}^{-1} = \tau_m^{-1} + \tau_c^{-1} \tag{2.21}$$

The recombination time for Langevin type follow the rules as $\tau_c << \tau_m$. This mechanism in solid-state physics, is distinguished using the relationship of the mean free path of optical photon emission, λ, with the thermal capture radius, r_c. The Langevin recombination rates has $\lambda << r_c$.

Thomson recombination described a system in ambient gas, where ion to ion recombination occurred, and the recombination rate is given by the following equation

$$R_{Tho} = \pi r_T^2 \left(\frac{8k_B\theta}{\pi m} \right)^{\frac{1}{2}} \left(\frac{4}{3} r_T \lambda Q_e N \right) \tag{2.22}$$

and the trapping radius, r_T

$$r_T = \frac{3k_B\theta}{2e^2} \tag{2.23}$$

where θ is the ambient gas temperature, N is the density of neutral number, Q_e is the electron-ion collision cross section, m is the mass of electron.

If an organic semiconductor has a very low mobility carrier ($\mu << 1$ cm^2/Vs) and the mean free path has a value of λ=10 Å which is lower than capture radius, $r_c \approx 200$ Å with $\varepsilon \approx 3$, the Langevin recombination model would become the most suitable model to explain the recombination process. Alternatively, the recombination process in organic devices

can be simplified as the flow of opposite elements towards each other due to Coulombic field effect. The recombination of both electron and hole lead to a charge-neutral excited state of the molecule.

2.3.2.4 Emission of Photon

The objective of the electroluminescence processes is to convert all the electrical energy into a photon, an emissive light. For OLED devices, ideally, the emission spectra must cover all the visible spectral range colour from blue to red, especially for the display technology and other optoelectronic devices. These emitted spectra give various shapes and characteristics due to their molecular properties. For instance, a broad spectrum emission maxima can be obtained from a disordered emitted molecule and the excited state of two-molecules (Adachi et al., 2001). Meanwhile, the narrow line emissions are coming from the lasing and microcavity effect in OLED structure (Melpignano et al., 2010) or from the reflected excitation of metal ions in organic complexes material (Li, 2011).

A very large Stokes shift (distance from absorption to emission of a molecule) is observed in the organic semiconductor, due to structural distortion of a molecule that facilitates the deep localization of the first excited singlet. The disordered structure of organic material leads to an extended long-wavelength and a larger width of emission reflected from a high density of defects in a structure that is not homogenous. By simply modifying the chemical structure (Ali et al., 2009), the emission colour from OLED devices can be tuned. The EL colour also can be changed by doping process (Li et al., 2007) where the dopant molecule has a small energy gap, and the host polymer has a wider energy gap.

2.4 Alq_3 Based OLED

For the fabrication of OLED devices, many organic compounds can be used as long as they have good optical and electrical properties. Most organic semiconductor compounds can be divided into small molecule and conjugated polymer groups. Small molecule compound referred to organic materials that have very low atomic molecular weight as opposed to the polymer materials. Small molecule materials can be used as either a hole transport materials, electron transport materials, and even emissive materials depending on their molecular structures and derivatives.

The small molecule compound that has been used for the fabrication of OLED devices in this work is Tris(8-hydroxyquinolinato)aluminium (Alq_3). This material was first reported by Tang and VanSlyke (1987) from Kodak Corp . Using Alq_3 and other types of small molecule compounds, many groups of researchers perform several experiments to understand more about small molecule compound. Alq_3 has a molecular structure of three 8-quinolate ligands that are distorted octahedrally and attached to the aluminium metal, wherein the solid-state; it would avoid the photoluminescence (PL) quenching. It has a T_g of 172°C (Higginson et al., 1998) and able to form an amorphous thin film using thermal evaporation deposition technique. Using the time-of-flight (TOF) measurement (Kepler et al., 1995), the charge carrier mobility of electron for Alq_3 is typically 1.4×10^{-6} $cm^2/(Vs)$, which is higher than the charge carrier mobility of holes which is typically 2.0×10^{-8} $cm^2/(Vs)$.

Organo-metallic chelate defined as materials containing compound which have bonding of ion and molecules between multiple ligand and metal ions becomes the single central atoms. Alq3 is a perfect example as shown in Figure 2.2(a) where Al becomes the single central atoms bonded to the conjugate base of three 8-hydroxyquinoline ligands. This organo-metallic chelate or Alq_3 shows good electron transport properties and

efficient emissive materials due to it's HOMO and LUMO energy level of -5.95eV and -3.00eV (Anderson et al., 1998), respectively. Using a doping method such as co-hosting the hydoxyquionaline with the phenanthroline derivatives (Choy et al., 2006) can improve the mobility of electron in Alq_3.

2.5 Summary

The chemical and physical properties of the organic material are closely related to the electroluminescence process in the OLED device. A suitable material for the electrode should also be considered. The alignment of energy level among the electrodes and the organic materials play a major role to achieve a highly efficient OLED device. Balancing the charge accumulation on the emission region may increase the possibility of exciton formation and better recombination process. In this work, research is focused towards a theoretical work represented by trap density, which can be manipulated/changed to achieve more and better efficient device.

CHAPTER 3: THEORETICAL STUDY ON THE CHARGE CARRIER TRANSPORT

3.1 Introduction

Since the success of first OLED devices fabrication by Tang and Vanslyke (1987), good and steady progress has been made to improve these devices for various real-world applications. Electrical and optical modelling of OLED devices often used to provide direction and detailed understanding of the physical processes governing the macroscopic device behavior. This enables rapid exploration of possible device parameters space.

Most theoretical or simulation models either focused on the electrical properties which consist of the charge carrier's injection profile, the charge carrier transport modelling, and the charge carrier recombination theory or the optical model which is the light output and the parameter involves include the recombination zone and radiative emission profile, exciton diffusion and absorption of the photons. This chapter focused on the electrical properties, specifically on the charge carrier transport. Theoretical studies on electrical properties have many restrictions and thus, some simplification are necessary. In this study, we shall consider the following:

i. field independent hole and electron mobility
ii. trapping phenomena is considered only within the charge transport
iii. anode and cathode provide ohmic contacts
iv. restriction to one or two organic layers

In this chapter, the trap phenomena in OLED devices and all the assumption used will be discussed in details. A theoretical explanation and discussion on the electrical properties of OLED devices require the inclusion of traps. This will be emphasized in this part of the research work.

3.2 Trap Density

Traps phenomena is an integral part of organic semiconductor since impurity generally exists in all organic matter or materials. Trap states assumed the charge carriers are trapped anywhere in a system until it recombines (surface or in the bulk). Trap density near the surface are referred to as shallow traps. Deep traps is defined as generation-recombination centres which capture/emit both electrons and holes and exist at the bulk. Recent studies have shown that trap density affects the performance of the device. Trap density at temperature ranging from 300-420 K, is proven to limit the diffusion of polaron pairs and excition, promoting the intersystem crossing within the device (Zhu et al., 2020). Shi et al. (2019) showed a correlation that post annealing at high temperature, ranging from 150 - 200°C would reduced trap density of devices and thus a lower turn-on voltage and much higher luminescence achieved. Lee et al. (2018) found that trapped electrons in Alq_3 devices increased hole transport and reducing the driving voltage, from using the analysis of capacitance-voltage and displacement current measurement. A theoretical study has pointed out that the large fluctuations in the transfer integral of thermal motion in the molecules resulting in a tail of trap states extending from the valence-band edge into the gap, and the band tail is temperature-dependent (Sleigh et al., 2009). Some experimental studies suggest that trap states due to the thermal motion of the molecules play a role in samples with a low trap density (Krellner et al., 2007;Haas et al., 2007; Pernstich et al., 2008). Tsai and Meng (2005) reported that traps could reduce the current generated from a fixed voltage, strongly increase the transient time, which causes slow carrier transportation in the device. Traps can also alter the recombination region close to the cathode and thus reduce external quantum efficiency and performance of the device.

Tsai and Meng (2005) highlight the importance of studying trap dependencies in charge transport in order to provide a foundation understanding of electroluminescence

(EL) mechanism in devices. In order to understand trap phenomena better, a clear definition of traps and its correlation with charge carrier transportation is needed. Subsection 3.2.1 will focus on the origin and definition of traps, and the subsequent section will focus on the current-voltage relationship.

3.2.1 Shockley-Read Hall Theory

Many researchers suggest that traps are caused by chemical impurities that were formed during the material's synthesis. The chemical impurities may develop surrounding structural defects by distorting the host lattice (Probst & Karl, 1975). Chemical impurities also tend to accumulate in regions with increased structural disorder (Pope & Swenberg, 1999) as well as at the surface of a crystal (Jurchescu et al., 2007).

In the basic principle of semiconductor physics and devices, Shockley-Read-Hall (SRH) theory of recombination describes trap as an allowed energy state within the forbidden bandgap (Neaman, 1992). It may also act as a recombination centre, capturing both types of carriers (electron and hole). Shockley-Read-Hall theory of recombination simply assumes that a single recombination centre or trap exist at energy E_t within the bandgap. At this single trap, any of the four basic processes would have occurred. In order to explain these processes, the trap is assumed to be an acceptor type, which is negatively charged when it is contained with electron and neutral when it does not contain an electron.

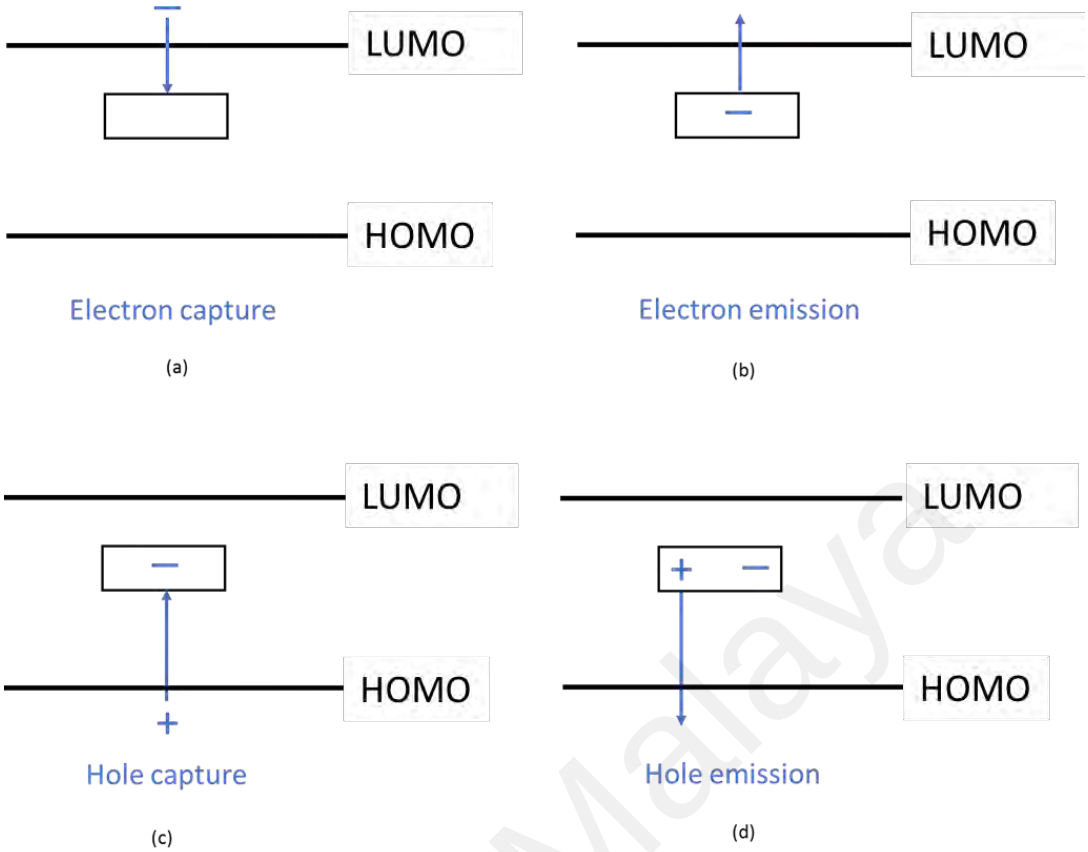

Figure 3.1: Four processes that occurred to charge carriers in trap states that exist in the bandgap.

In Figure 3.1, the minus sign (-) represents the electron charge carrier while the plus sign (+) represents the hole charge carrier. The rectangular box in the middle represents the trap level (localized states) that exist in a bandgap. The arrow shows the direction where the charge carrier comes from and goes to. In the organic semiconductor field, the term lowest unoccupied molecular orbital (LUMO) is used instead of conduction band whereas highest occupied molecular orbital (HOMO) replaces valence band.

Figure 3.1(a) shows the capture of an electron from the conduction band by an initially neutral empty trap. Figure 3.1(b) shows the emission of an electron that is initially occupying a trap level back into the conduction band. It is also can be referred to as the inverse of the process in Figure 3.1(a). Figure 3.1(c) is the capture of a hole from the valence band by a trap containing an electron. The process could also be considered as

the emission of an electron from the trap into the valence band. Figure 3.1(d) represents the emission of a hole from a neutral trap into the valence band, which is the inverse of the process in Figure 3.1(c). The process could also be considered as capturing an electron from the valence band.

From the SRH theory, the rate of an electron from the conduction band captured by traps is assumed to be proportional to the density of electrons in the conduction band, also to the density of empty trap states. The electron capture rate can be written as (Neaman, 1992)

$$R_{cn} = C_n N_t (1 - f_F(E_t)) n \tag{3.1}$$

where

R_{cn} = capture rate ($cm^{-3}s$)

C_n = constant proportional to electron-capture cross section

N_t = total concentration of trapping centers

n = electron concentration in the conduction band

$f_F(E_t)$ = Fermi function at the trap energy

E_t = trap energy

The Fermi function at the trap energy is given by

$$f_F(E_t) = \frac{1}{1 + \exp\left(\frac{E_t - E_F}{kT}\right)} \tag{3.2}$$

which is the probability that a trap will contain an electron. The function (1-$f_F(E_t)$) would be the probability that the trap is empty. In SRH theory, the rate which electron is emitted from the filled traps back into the conduction band, is proportional to the number of filled traps, so that

$$R_{en} = E_n N_t f_F\left(E_t\right) \tag{3.3}$$

where

R_{en}=emission rate ($cm^{-3}s$)

E_n = energy gap of the trapped electron

$f_F(E_t)$ = Fermi function of the trapped energy

In thermal equilibrium, rate of electron capture from conduction band and rate of electron back into the conduction band must be equal,

$$R_{en} = R_{cn} \tag{3.4}$$

and

$$E_n N_t f_{F0}\left(E_t\right) = C_n N_t\left[1 - f_{F0}\left(E_t\right)\right] n_0 \tag{3.5}$$

The thermal-equilibrium Fermi function is denoted by f_{F0}. In thermal equilibrium, value of the electron concentration in the capture rate term is the equilibrium value n_0. Applying Boltzmann approximation for the Fermi function, E_n becomes

$$E_n = n' C_n \tag{3.6}$$

n' is defined as

$$n' = N_c \exp\left[\frac{-(E_c - E_t)}{kT}\right] \tag{3.7}$$

Parameter *n'* is equivalent to electron concentration that would exist in conduction band if the trap energy E_t coincide with the Fermi energy E_F. In non-equilibrium, excess electron exists, the net rate at which electron are captured from the conduction band is given by

$$R_n = R_{cn} - R_{en} \tag{3.8}$$

which is the difference between the capture rate and emission rate. Combining both Equation (3.1) and Equation (3.3) with Equation (3.8) yields

$$R_n = \left[C_n N_t (1 - f_F(E_t))n\right] - \left[E_n N_t f_F\left(E_t\right)\right] \tag{3.9}$$

In this equation, *n* is the total electron concentration, including the excess electron concentration. The remaining constants and term in Equation (3.9) are the same as defined previously, and the Fermi energy in the Fermi probability function needs to be replaced by the quasi-Fermi energy for electrons. The constant E_n and C_n are related through Equation (3.6), so the net recombination rate can be written as

$$R_n = C_n N_t \left[n\left(1 - f_F\left(E_t\right)\right) - n' f_F\left(E_t\right)\right] \tag{3.10}$$

Considering process (c) and (d) in Figure 3.1 of the recombination theory, the net rate for holes that are captured from the valence band is given by

$$R_p = C_p N_t \left[p f_F\left(E_t\right) - p'(1 - f_F(E_t))\right] \tag{3.11}$$

C_P is a constant proportional to hole capture rate and *p'* is given by

$$p' = N_v \exp\left[\frac{-(E_t - E_v)}{kT}\right] \tag{3.12}$$

In a semiconductor which the trap density is not too large, the excess electron and hole concentration are equal, and the recombination rates of electron and holes are also equal. Solving the Fermi function by setting Equation (3.10) equal to Equation (3.11) will lead to the derivation of Equation (3.13)

$$f_F(E_t) = \frac{p'C_p + C_n}{C_n(n+n') + C_p(p+p')} \tag{3.13}$$

Considering thermal equilibrium, which $np=n_0p_0=n_i^2$, where n_0 and p_0 is the thermal equilibrium concentration of electron and holes respectively, Equation (3.10) and Equation (3.11) becomes $R_n=R_p=0$.

$$R_n = R_p = \frac{C_n C_p N_t (np - n_i^2)}{C_n(n+n') + C_p(p+p')} \equiv R \tag{3.14}$$

Equation (3.14) represents the recombination rate of electron and holes due to the recombination centre at $E=E_t$. R is the recombination rate of excess electrons and holes, which in the case of thermal equilibrium, $R=0$. For the case of non-thermal equilibrium, R is given by

$$R = \frac{\delta n}{\tau} \tag{3.15}$$

where

δ n = excess carrier concentration

τ = lifetime of excess carrier

3.2.2 Nanocrystalline Semiconductor Theory

In nanocrystalline semiconductors, trap phenomena contribute to different properties of the materials and can modify some parameters of the device (Korkin & Rosei, 2008). In comparison, a single trap in a nanocrystal of a thousand atoms represents trap concentration much greater than any value attained in bulk semiconductors.

Non-equilibrium carriers (electron and holes) in bulk semiconductor materials can be generated by processes such as light absorption, high electric field, carrier injection through a barrier, or irradiation with high energy particle. The non-equilibrium free carrier involved in the electrical transport of a nanocrystalline semiconductor.

In the case of excitation by light absorption, the supplementary current due to the non-equilibrium carriers is called photocurrent. The injection current is generated by carriers injected through the Schottky barrier or p-n junction. After the process of generating non-equilibrium carriers is terminated, the system returns to equilibrium due to the annihilation of the electron-hole pair by recombination. The relaxation in a time of the system follows an exponential law toward the thermodynamic equilibrium (Bube, 1992).

In the case of recombination of both free carriers (electron in the conduction band and hole in the valence band), the annihilation process is called band-to-band recombination. If one of the carriers captured on a localized state (it has a fixed position in the device) and the other one is free, this is called recombination on localized states. By recombination process, the byproduct would be an amount of energy released by the emission of either a photon (radiative recombination) or a phonon (non-radiative recombination), or a secondary electron (Auger recombination).

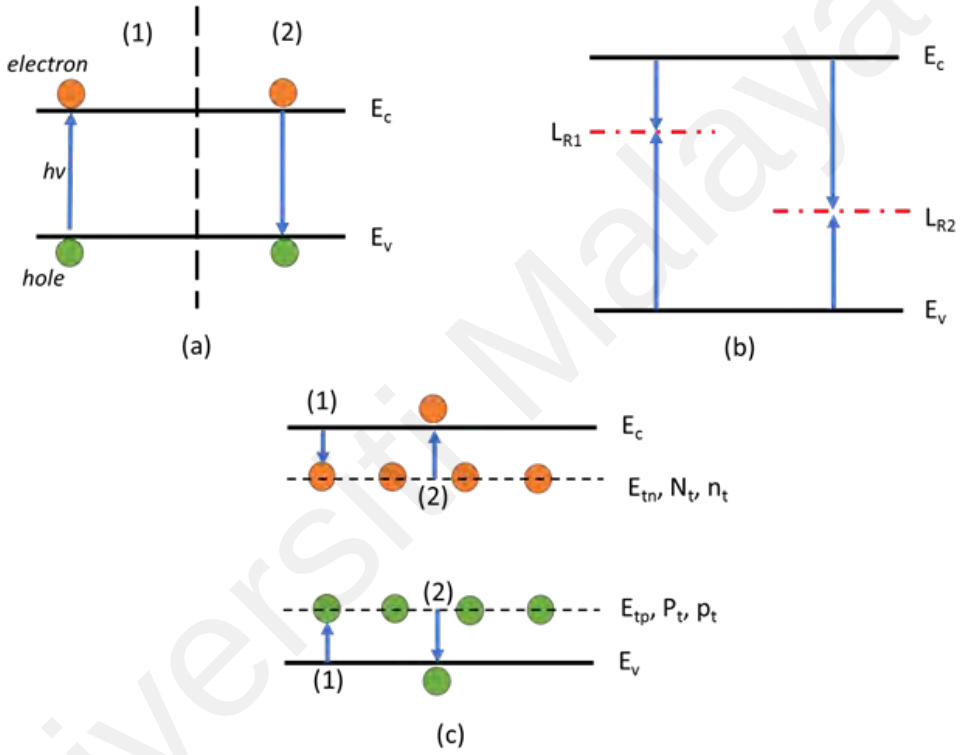

Figure 3.2: Transition process occurring to charge carriers in the device.

Figure 3.2 represents the transition process. Electron charge carrier is represented with an orange dot while hole charge carrier with green dot. In Figure 3.2(a), process (1) known as intrinsic absorption. It occurs when hole interacts with electron and excites into a higher energy level and the energy released, $E = \hbar v$. Process (2), band-to-band recombination occurs when an electron moves from its conduction band states to valence band state and interact with a hole.

Note that, the charge carrier moved from a higher energy level to a lower one, the opposite of process (1). Figure 3.2(b) illustrates multiple localized states that act as a recombination centre, $L_{R1,}$ and L_{R2}. The energy level of L_{R1} is much higher than L_{R2}, closer to the conduction band and L_{R2} energy level is closer to the valence band. Figure 3.3(b) illustrates localized states known as trapping centre. Each trapping centre captures different species of charge carrier, one for electron and the other for holes. E_{tn} denotes the electron trap energy level, N_t defined as the electron trap density of states while n_t is the trapped electron charge carrier density. E_{tp}, P_t and p_t is the same definition but for holes charge carrier.

Figure 3.2(b) shows the recombination process on localized states, L_R. On level L_{R1}, one electron is first captured and annihilated by a hole capture. For level L_{R2}, a hole is first captured and then annihilated by electron capture. For the case shown in Figure 3.2(c), the trapping and de-trapping processes are presented for two kinds of traps, one for electron and the other for holes. The trapping of either holes or electrons represented by (1) and the de-trapping is (2).

The trapping level is characterized by the following parameters: activation energy ($\Delta E_{tn}=E_c-E_{tn}$ for electron traps and $\Delta E_{tp}=E_{tp}-E_v$ for hole traps), the capture cross-section (ς_n for electrons and ς_p for holes), the trapping center concentration (N_t for electrons and P_t for holes), and the trapped carriers (electron and holes) concentration ($n_t \leq N_t$ and $p_t \leq P_t$). The trapped carrier concentration represents the concentration of the trapping centre occupied by electrons or holes. The rate of the capture process of electrons (with concentration n) on localized states (with concentration N_t), R_n is given by Equation (3.16).

$$R_n = c_n n N_t \tag{3.16}$$

where

$$c_n = \varsigma_n \tilde{\nu}_e \tag{3.17}$$

ζ_n = capture cross section

and

$$\tilde{v}_e = \sqrt{\frac{3k_B T}{m_e^*}} \tag{3.18}$$

$\tilde{v}_e$ is defined as the thermal velocity of electrons (Bube, 1992; Ryvkin, 1964). A similar expression can be written for the holes, given by Equation (3.19). The lifetime of the free non-equilibrium carrier by definition is the meantime during which the carrier is free before recombination and is given by the Equation (3.20) for electron and Equation (3.21) for holes.

$$R_p = c_p p P_t \tag{3.19}$$

$$\tau_n = \frac{1}{c_n N_t} \tag{3.20}$$

$$\tau_p = \frac{1}{c_p P_t} \tag{3.21}$$

If the captured carrier is released in the band, the capturing centre is called a trap. Then, the capture process is simply trapping, and the release process is called de-trapping. The de-trapping rate is defined similarly with the trapping rate as in Equation (3.22) where N_{ct} is the effective density of states in the conduction band containing the trapped charge carrier. For Equation (3.23), N_c is the effective density of states in the conduction band

and ΔE_{tn} is the depth of trapping level into the bandgap measured from the edge of the conduction band (trap activation energy). If $R'_n > R_n$, the capturing centre act as a trap and if $R_n > R'_n$, the capturing centre act as a recombination centre.

$$R_n^{'} = c_n n_t N_{ct} \tag{3.22}$$

$$N_{ct}(T) = N_c(T)\exp\left[-\frac{\Delta E_{tn}}{k_B T}\right] \equiv 2\left(\frac{m_e^* k_B T}{2\pi\hbar^2}\right)^{\frac{3}{2}} \exp\left[-\frac{E_c - E_{tn}}{k_B T}\right] \tag{3.23}$$

In Equation 3.23, the terms used are defined as follows:

N_{ct}= effective density of states in the conduction band containing the trapped charge carrier

m^*_e= relative mass of electron

$\hbar$ = reduced Plank constant

k_B= Boltzmann constant

3.3 Current-Voltage Characteristic

The trap density of the OLED device can be related to its current-voltage characteristic. The charge carrier transport in OLEDs can be quantified or described by the current-voltage measurement. Transportation phenomena in the steady-state conduction occurred when neither the number of charge carrier nor the local electric field changed with respect to time. The current is given by

$$J = nq\mu E \tag{3.24}$$

n refers to charge carrier concentration, q is the Coulomb electric charge, μ is the mobility of the charge, and E is the electric field. In an ideal ohmic electrodes contact,

there is no potential barrier for injection; thus, the ohmic electrode is capable of providing an infinite supply of charge carriers. It is possible to derive the trap-free dielectric, so-called Child's law by making use of the Poisson's equation (Lampert & Mark, 1970):

$$J = \frac{9}{8}\varepsilon\mu\frac{V^2}{d^3} \tag{3.25}$$

where ε is the dielectric constant, V is the applied voltage, and d is the sample thickness. The origin of deviation from Ohm's law is that the solid is unable to transport all the injected charge. Accumulation of charges may occur, limiting the conducting current. This effect is known as space charge limited current (SCLC).

If traps exist in the solid, the SCLC will decrease by several orders of magnitude (Rose , 1955). Lampert et al., (1959) argues that neither field distribution or the charge density should be altered by trapping. Thus, the relationship between current and voltage needs to be modified by introducing a trap limiting parameter, θ, that establishes the proportion of the trapped charge to the free charge. The current density is then rewritten to (Bonham, 1973):

$$J = \frac{9}{8}\varepsilon\mu\theta\frac{V^2}{d^3} \tag{3.26}$$

where

$$\theta = \frac{n}{n + n_t} \tag{3.27}$$

where n_t is the density of trapped charges and n is the density of mobile charge carriers. In a real case, traps are more likely to be distributed in energy rather than exist at discrete levels (Sworakowski, 1970). The injected carriers are expected to be trapped, shifting the quasi-Fermi level upwards. Looking at an exponential density of traps, and under the

approximation that all the trapping states are filled below the Fermi level, the current-potential characteristic can be written as (Mandoc et al., 2007)

$$J = q\mu N_c \left(\frac{\varepsilon}{qH_t}\right)^{\ell} \left(\frac{\ell}{\ell+1}\right)^{\ell} \left(\frac{2\ell+1}{\ell+1}\right)^{\ell+1} \frac{V^{\ell+1}}{d^{2\ell+1}} \tag{3.28}$$

with

$$\ell = \frac{T_c}{T} \tag{3.29}$$

where q refers to the Coulomb electric charge, μ is the mobility of the charge carrier, ε is the dielectric constant, N_C is the effective density of states in the transport level, H_t is the effective density of traps, T_c is the characteristic trap temperature, T is the operating temperature, and d is the thickness of the device.

$$H_t = \frac{2\varepsilon_s \varepsilon_0 V}{qd^2} \exp\left[\frac{T\left(\frac{\ln \mu N_c qV}{2d} - \ln J\right)}{T_c}\right] \tag{3.30}$$

Equation (3.30) show that H_t depends on voltage and current density. Thus, H_t value can be calculated from the current-voltage characteristic of the devices. More details for the re-arrangement and further application on the equation is discussed in Chapter 5 and reported in Zaini et al. (2016). The equation is used to estimate the trap density of fabricated OLED devices in Chapter 6.

3.4 Summary

Trap density phenomena are very crucial and heavily affect the performance of the OLED devices. Definition and origin of trap density are presented and discussed in this chapter. From the theory, a mathematical expression on trap density is presented in the

form of Equation 3.30. From Equation 3.30, certain parameter values are required in order to quantify the value of trap density. In Chapter 4, details on the device fabrication and characterization method are discussed in order to obtain all the necessary parameters needed to estimate the trap density of the devices.

CHAPTER 4: EXPERIMENTAL METHOD

4.1 Introduction

The prime objective in this experimental part was to fabricate functional OLED devices in order to obtain all the parameters needed and complement the theoretical studies in the previous chapter. The first part of this research starts with the preparation of substrate and the organic solvent used in the process. The subsequent section describes the formation of the thin-film by using the solution processing of the spin coating technique and the fabrication of device electrode using the thermal evaporation technique. Finally, the experimental setup for both thin-film and device characterization are described. For the thin film, the characterization technique used is limited to thickness measurements only (profiler measurement). No morphological studies are done on the thin film; thus, a uniform thin film formation is assumed instead. Surface morphology is unnecessary since it is not related to the objective in Chapter 1. The materials and the structure for the devices used in this work has been thoroughly researched including the surface morphology. Trap density analysis related to surface morphology has also been reported. In this work, two types of OLED has been prepared. One is the single layer OLED containing Alq_3 as the emissive layer (OLED A) and the second type is the single layer but with poly-TPD added as the HTL (OLED B). For the fabricated OLED devices, the only characterization techniques used was the measurement of current-voltage-luminescence (I-V-L).

4.2 Preparation of Pre-Patterned ITO

Pre-patterned ITO substrate, which consists of glass and Indium Tin Oxide (ITO) were used for the fabrication of thin-film and OLED devices. An ITO-coated on top of a glass substrate is used as an anode in OLED fabrication due to its characteristic as a transparent metal thin film and also having suitable (high) work function (Wang et al., 2007). Higher work function allows the hole charge carrier to be easily injected from the ITO material

to travel through the organic thin-film when the voltage applied is sufficient (to overcome the barrier height potential) as explained in Chapter 2. The values for the barrier height potential solely depends on the HOMO level of the respective organic materials used. The substrate preparation is an essential method when it is done properly, able to avoid contamination during the thin film formation and devices. A suitable substrate preparation process could also control the size of an active area of OLED devices.

The details for the pre-patterned ITO cleaning procedure are described below:

i. In order to make sure pre-patterned ITO free from contamination (dust and small particles), the substrates were immersed in an ultrasonic bath for 30 minutes in a beaker containing soap water.
ii. The substrates were then rinsed multiple times with distilled water in order to remove the remaining soap water before being immersed in an ultrasonic bath for 30 minutes in a beaker containing distilled water.
iii. The substrates were purged to dry using nitrogen gas before being immersed in an ultrasonic bath for 30 minutes in a beaker containing acetone to remove the contamination of the non-polar type.
iv. The substrates were purged again to dry using nitrogen gas before being immersed in an ultrasonic bath in a beaker containing isopropyl alcohol (IPA) for 30 minutes in order to remove the contamination of the polar type.
v. The substrates were dried in an oven for 1 hour with a temperature of 80°C.
vi. The substrates finally purged with nitrogen gas and now ready to be used.

4.3 Preparation of Organic Solution

The materials used for the emissive layers was Tris(8-hydroxyquinoline)aluminium (Alq_3), purchased from Merck and used without further purification. The Alq_3 solution was prepared by dissolving the powdered materials in a chloroform solvent ($CHCl_3$). The concentration of the Alq_3 solution was prepared at 15 mg/ml in order to get approximately the film thickness of 70 nm. To ensure the Alq_3 materials dissolved completely, the solution was stirred by using a magnetic stirrer bar at 700 rpm with a calibrated temperature setting of 40°C for 1 hour long. All of the solution preparation processes were performed in a clean-room environment at atmospheric pressure.

4.4 Fabrication Process of Thin-Film

The spin coating technique is used to fabricate thin films and OLED devices. A spin coater with model number Laurell WS-400B-6NPP/LITE was used. The spin coater system is operated by applying high-pressure nitrogen gas to the motor system. A nitrogen tank cylinder with a capacity of 50L connected to the spin-coater system by a plastic host. The bottom of the substrate holder was connected to a rotary pump system. The rotary pump was set to vacuum in order to hold the substrate properly in place and ensuring the solution is uniformly spread on top of the substrate while the spin coating process was performed. The system itself has a safety mechanism where the instrument is unoperational if the nitrogen gas and vacuum pressure were not sufficiently supplied.

The parameters for spin coating were determined to obtain a specified film thickness. The duration and spin speed were set to 30 s and 2000 rpm, respectively in order to get 70 nm film thickness (measured) for an Alq_3 solution prepared at 15 mg/ml concentration. The fabrication process for the thin-film is described in Figure 4.1.

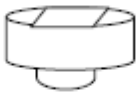

1) A glass substrate that has been cleaned was placed on the platform.

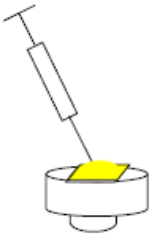

2) Approximately 0.1 ml of Alq_3 solution was pipetted onto the glass substrate.

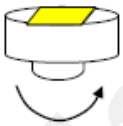

3) The spin coater was operated at 2000 rpm for 30 s.

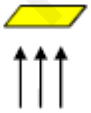

4) The spin coated film was thermally annealed at 60ºC for 30 minutes to remove residual solvent.

5) The prepared thin-film is ready for characterization.

Figure 4.1: Thin-film fabrication process utilizing the spin coating technique.

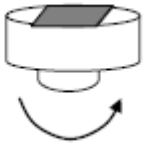

1) PEDOT: PSS was spin coated onto a pre-patterned ITO substrate set at 2000 rpm and 30 s.

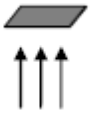

2) The PEDOT:PSS film was annealed at 120°C for 30 minutes to remove residual solvent.

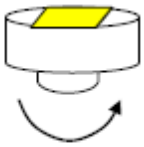

3) The Alq_3 solution was spincoated onto PEDOT: PSS film set at 2000 rpm for 30 s.

4) The spin coated film was annealed at 60°C for 30 minutes to remove residual solvent.

5) 100 nm thickness of an aluminum was deposited as the electrode on top of the thin-film.

Figure 4.2: An OLED device fabrication process.

Figure 4.2 described the overall process of an OLED device fabrication analyzed in this work. Initially, the spin coating process of PEDOT:PSS solution were done on top of the ITO pre-patterned substrate to form a thin-film layer with a spin speed of 2000 rpm for 30 s to form a hole injection layer (HIL) with a measured thickness of 40 nm. The PEDOT:PSS layer act as a hole injection layer (HIL) because of its HOMO level is higher than the electron affinity of the ITO substrate (Petr et al., 2004). Aside from being used as a HIL, PEDOT:PSS can also treat and refined the surface roughness of the pre-

patterned ITO substrate that is high after the cleaning process (Kim et al., 1998; Wantz et al., 2005). Aluminium (Al) was used as the electrode (cathode) due to their work function which is much lower when compared to ITO which functioned as the anode (Lee et al., 2006; Lü et al., 2011). After all the spin coating process of organic materials was completed, an Al electrode was deposited using the thermal evaporation technique on top of the PEDOT:PSS/Alq_3 layer using a thermal evaporation technique.

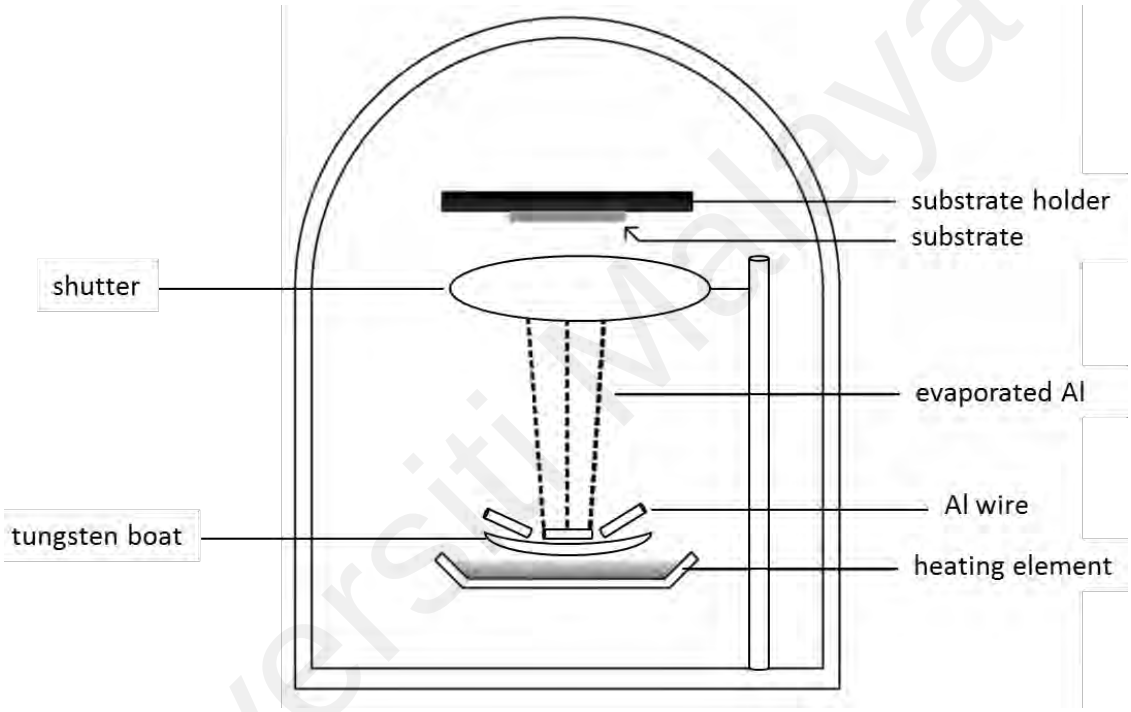

Figure 4.3: Simplified version of a typical thermal evaporation deposition system.

The thermal evaporator system diagram is shown in Figure. 4.3. The deposition process of the Al electrode was done in a vacuum environment with a measured pressure of 6.4 X 10^{-4} Pa. A few pieces of Al wire were put inside of a tungsten boat that functioned as a heating element. The displayed current of values ranging from 65 to 90 was used to heat the tungsten boat until the Al wires started to melt and ready to be evaporated. A shutter was opened to allow the evaporated Al flows upwards to the samples and a quartz sensor was used to count the rate of evaporation and thickness of the deposited Al which

was displayed through a thickness monitor. The evaporation rate was maintained around less than 4 nm/s to form a uniform Al electrode and at the same time avoiding the particles from diffusing into the organic layer. After the intended thickness was achieved, the shutter was closed, and the current was reduced slowly to zero.

4.5 Measurement of Thin-Film Thickness

A profilometer with model number KLA Tencor P-6 was used to measure the thickness of all the thin-film fabricated in this work. The KLA Tencor P-6 profiler system is also extremely useful for surface topography analysis.

The P-6 profilometer is suitable to be used for any substrates with size up to 150 mm. The principle of the film measurement used by P-6 profilometer was the steps height difference method. The measurement is done between the thin-film layer and the substrate (base). Figure 4.4 shows the example of an actual measurement for determining the thickness of a thin-film. The thin-film was scratched carefully in a straight line to form a different height. When the profilometer measurement is currently being run, the profiler tip will move in the given direction, and the surface profile of the sample is shown in the graph of step height versus distance. The thickness is then calculated from the step height. It is very important to note that for this particular model of profilometer has a limit of measuring thin-film no less than 10 nm; thus, the error limit in measurement would be ±10 nm. The yellow and purple rectangular represents the thin-film and glass substrate layer, respectively.

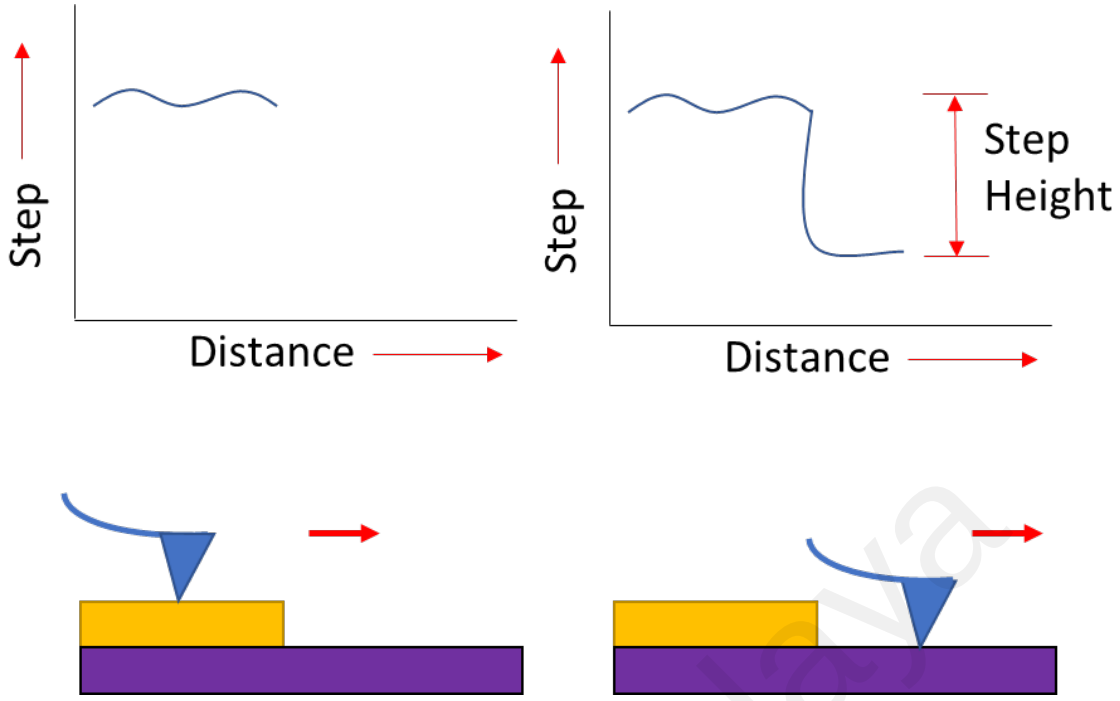

Figure 4.4: The measurement of film thickness using the step height difference method.

4.6 Characterization of an OLED Device

The current-voltage-luminance (I-V-L) measurement of the devices was carried out using a Keithly 2400 source measurement unit (SMU) together with a Konica Minolta CS-200 chromameter. The I-V-L measurement set-up is shown in Figure 4.5. CS-200 chromameter is used to record and measure the luminance, and the chromaticity values are comparable to spectroradiometers. The measurement of light sources is done by the instrument using three sensors of red, green and blue. The sensor is highly sensitive and quite similar to the human eye sensitivity towards light. The precision of reading is still limited even though the sensors are highly sensitive because of the filters used. The measured spectra of the light must be calculated mathematically using the spectral sensitivity characteristics where the colour matching function is used in order to rectify and correct this problem.

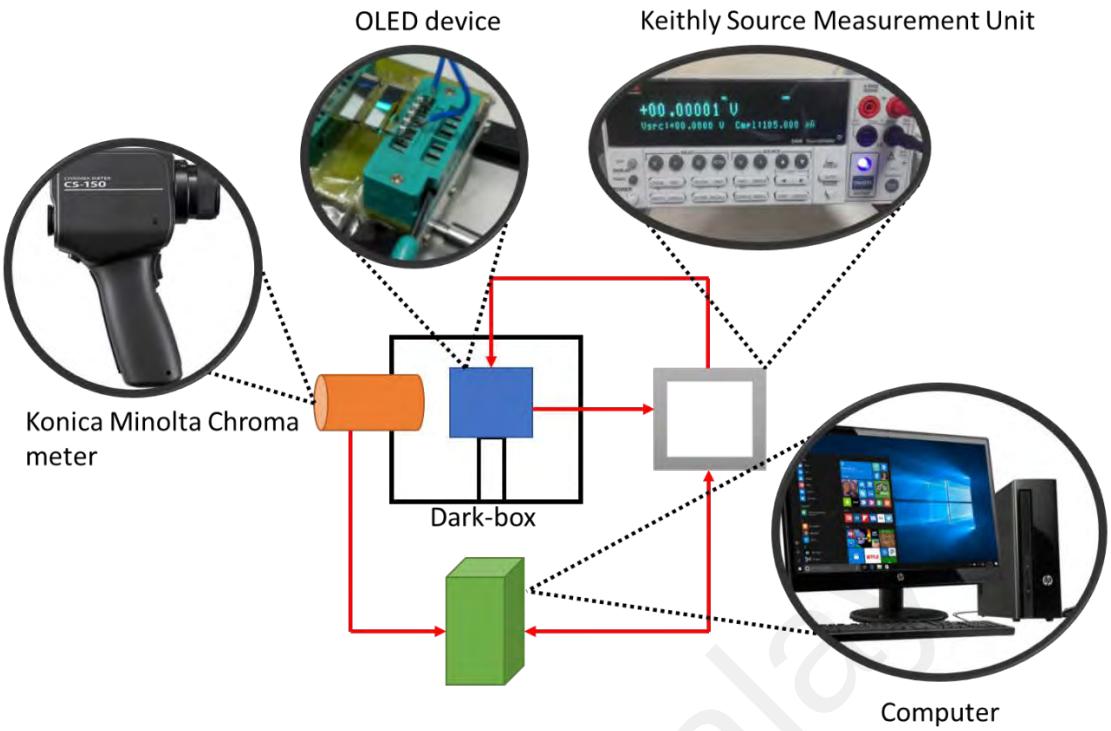

Figure 4.5: Experimental setup for the I-V-L measurement of the OLED devices.

The mathematical calculation of the measured spectra corresponds to the sensitivity of a human eye; thus are precisely determined. The CS-200 can measure in the range of brightness from 0.01 cd/m^2 to 200,000 cd/m^2. National Instrument Labview was used as an interface to control the Keithley SMU and the CS-200 via a computer where all of the measured data displayed and saved at the same time in a spreadsheet.

The Keithley 2400 SMU was used to control the voltage supplied to the OLED device and also measured and record the current as the output. The input voltage was varied from 0 to 20 V with a voltage increment of 0.5 V. The time interval between each point of measurement was set to be exactly 0.1 s. The devices were put in a dark-box connected with the CS-200 lens to eliminate the possibility of the surrounding light affecting the measurement and results. All measurements were performed in a room-

temperature environment with repetition of three times to ensure the validity and the reliability of data obtained.

From the device characterization, the current-voltage-luminescence (I-V-L) obtained needed to be converted to the standard unit used for OLED devices, which is the current density, J (A/m^2). Current density, J is given by the following equation.

Current density,

$$J = \frac{I}{A} \tag{4.1}$$

where I is the current in Ampere and A is an active area in a meter square. In this particular research work, device efficiency is not discussed and analyzed since the main objective of this research is to complement the theoretical work established as discussed in Chapter 3.

4.7 Summary

OLED devices were fabricated using a spin coating technique for the organic thin-film and thermal evaporation for the Al electrode part. The characterizations of the OLED devices were performed to obtain the current and the luminescence of the device as a much-needed parameter to complete the study.

CHAPTER 5: DETERMINATION OF TRAP DENSITY IN OLEDS FROM CURRENT-VOLTAGE ANALYSIS

5.1 Introduction

In Chapter 3, Equation 3.30 is established from the theoretical study as a simplistic method to estimate the trap density of an OLED device using only its current-voltage characteristic. Kumar et al. (2003) proposed a similar technique to estimate trap density from the current-voltage relationship also, but it involved the value of device temperature to be varied. Horowitz et al. (1995) technique required repeated measurement of trap DOS for the different operating temperature of devices plotted on the same graph, and the value where it coincides with each other is the trap DOS. The method proposed in this thesis emphasized on estimating the trap density with a single measurement of the current-voltage characteristic under the consideration that the device is working in normal room temperature. The equation used in this chapter is to estimate the trap density of single-carrier devices, which consist of an Electron Only Device (EOD) and Hole Only Device (HOD). The result then was compared with other people work (method) to demonstrate the equation used is valid and reliable.

5.2 Trap Density for Single-Carrier Devices

Single carrier devices allow either hole only or electron only travels as the current through the device. Electron-hole pair (exciton) does not exist in EOD or HOD; thus, no luminescence can be observed. EOD and HOD can provide useful information with regards to the nature of organic emissive material itself whether its favour electron charge carrier transport more than hole charge carrier transport and vice versa.

5.2.1 Device Structures of EOD and HOD

EOD and HOD with two different type of organic materials Poly(9,9-dioctylfluorene-alt-benzothiadiazole) (F8BT) (Müllen & Scherf, 2006) and 2-Methoxy-5-(3',7'-

dimethyloctyloxy)-benzene-1,4-diacetonitrile (OC_1C_{10}-PPV) (Lawrence et al., 2002). The next subsection would discuss in details on how the structure are constructed to only allow one type of carrier in the device and how their current-voltage relationship are being used to calculate and estimate their respective trap density.

Figure 5.1 shows the structure of HOD and EOD with F8BT as organic material, while Figure 5.2 shows the device structure of HOD and EOD with OC_1C_{10}-PPV as organic materials, respectively.

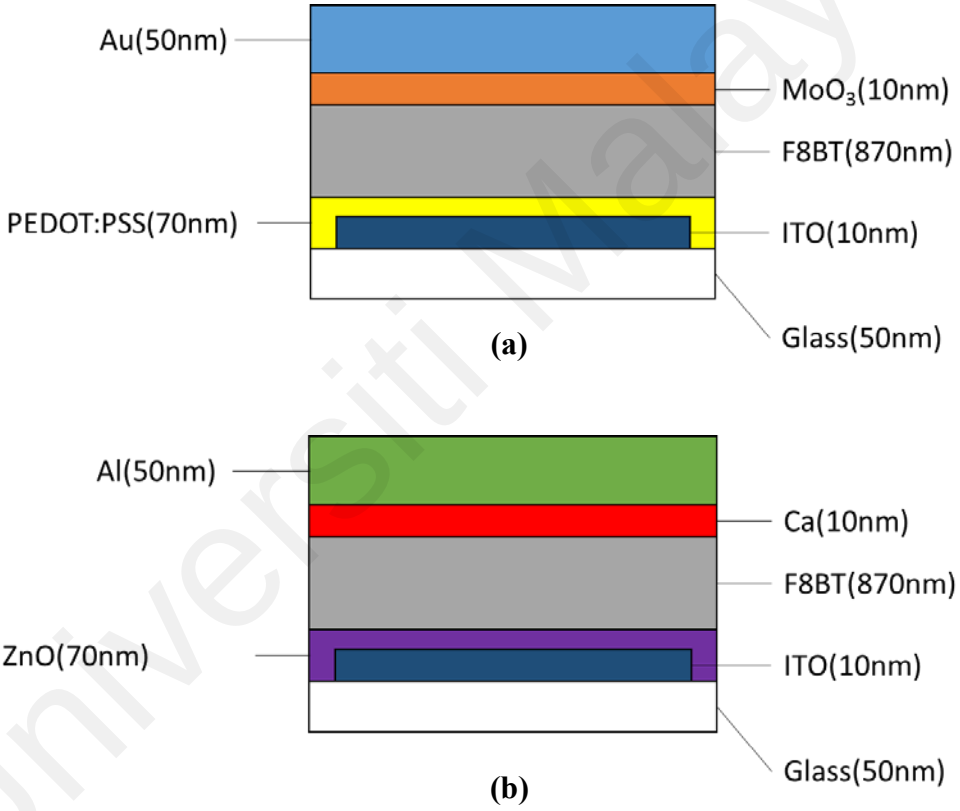

Figure 5.1: Structure of F8BT (a) Electron Only Device (EOD) and (b) Hole Only Device (HOD).

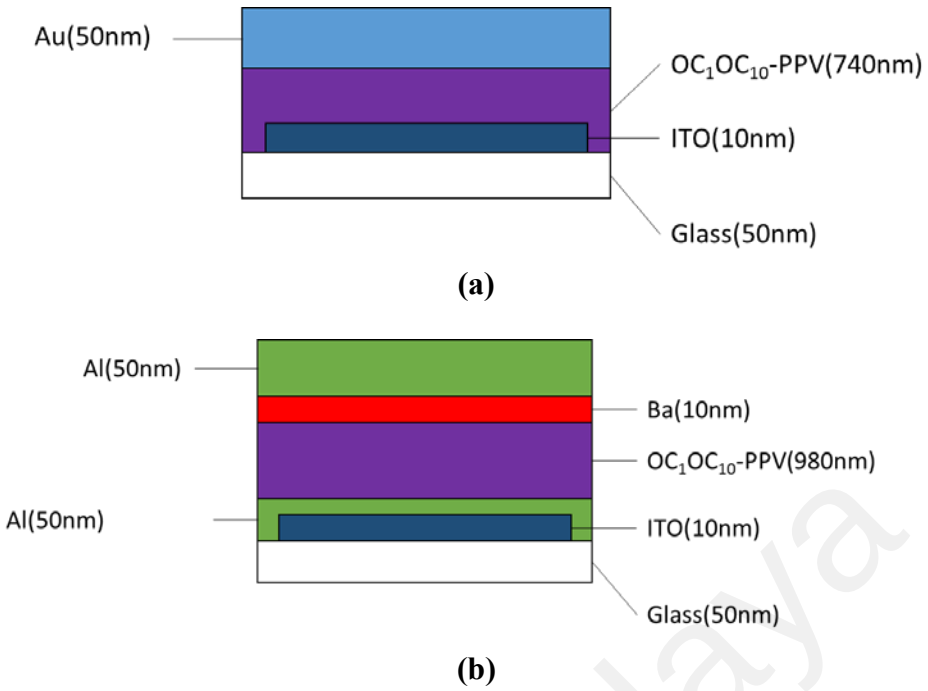

Figure 5.2: Structure of OC_1C_{10}-PPV (a)Electron Only Device (EOD) and (b) Hole Only Device (HOD).

5.2.2 Basic Working Principle of EOD and HOD

The basic working principle of each EOD and HOD for both materials is quite easy to understand. The energy band diagram would be able to explain the working principle of the devices.

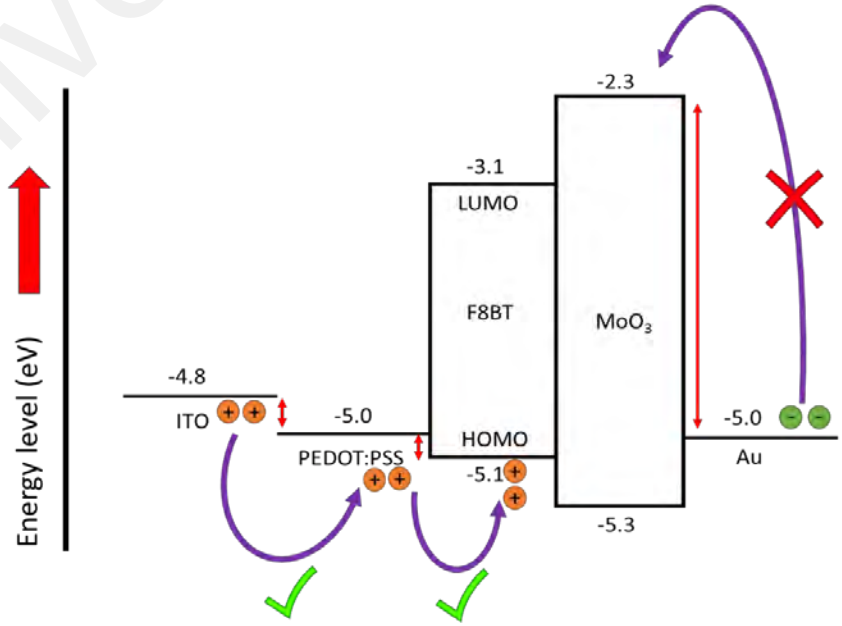

Figure 5.3: Energy band diagram for Electron Only Device (EOD) in F8BT device.

Figure 5.3 and Figure 5.4 shows the EOD and HOD energy band diagram for F8BT based material. In Figure 5.3, Molybdenum trioxide (MoO_3) is commonly used as a hole injection layer (HIL) or hole transport layer (HTL) in an organic device. When it is sandwiched in between F8BT and gold (Au) as the cathode, MoO_3 effectively becomes Electron Blocking Layer (EBL). Since Au work function is much higher than Indium-Tin Oxide (ITO), only holes are allowed to be injected into the device.

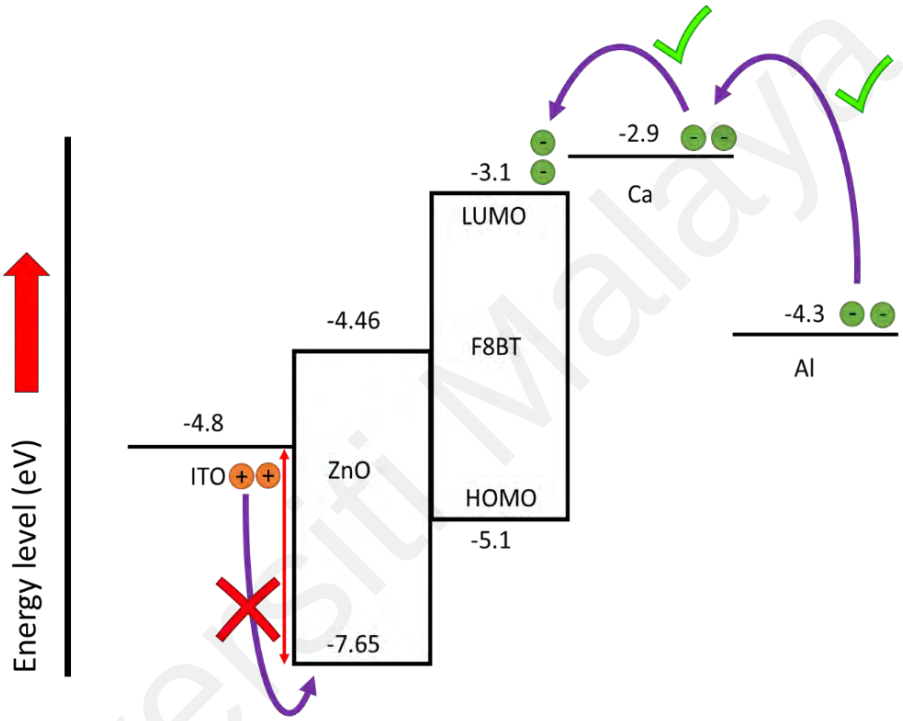

Figure 5.4 : Energy band diagram for Hole Only Device (HOD) in F8BT device.

Zinc Oxide (ZnO) is well known as highly conductive in thin-film and commonly used as Electron Transport Layer (ETL). In Figure 5.4, ZnO becomes Hole Blocking Layer (HBL), only allowing the electron to be transported. The low work function value of Calcium (Ca) favours electron more to be injected at the Al cathode. The same concept

applied to OC_1C_{10}-PPV devices. Figure 5.5 and Figure 5.6 shows the energy band diagram for EOD and HOD for OC_1C_{10}-PPV based material.

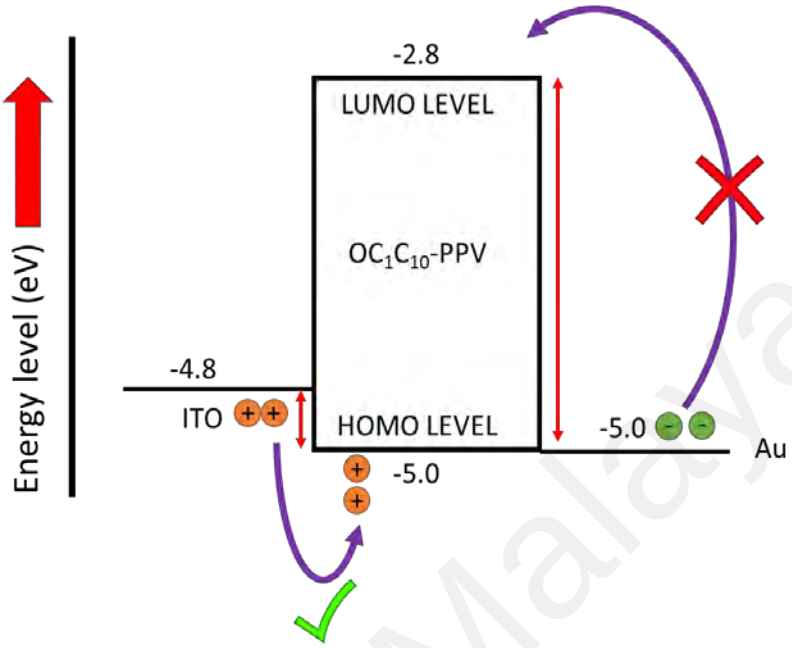

Figure 5.5: Energy band diagram for Hole Only Device (HOD) in OC_1C_{10}-PPV device.

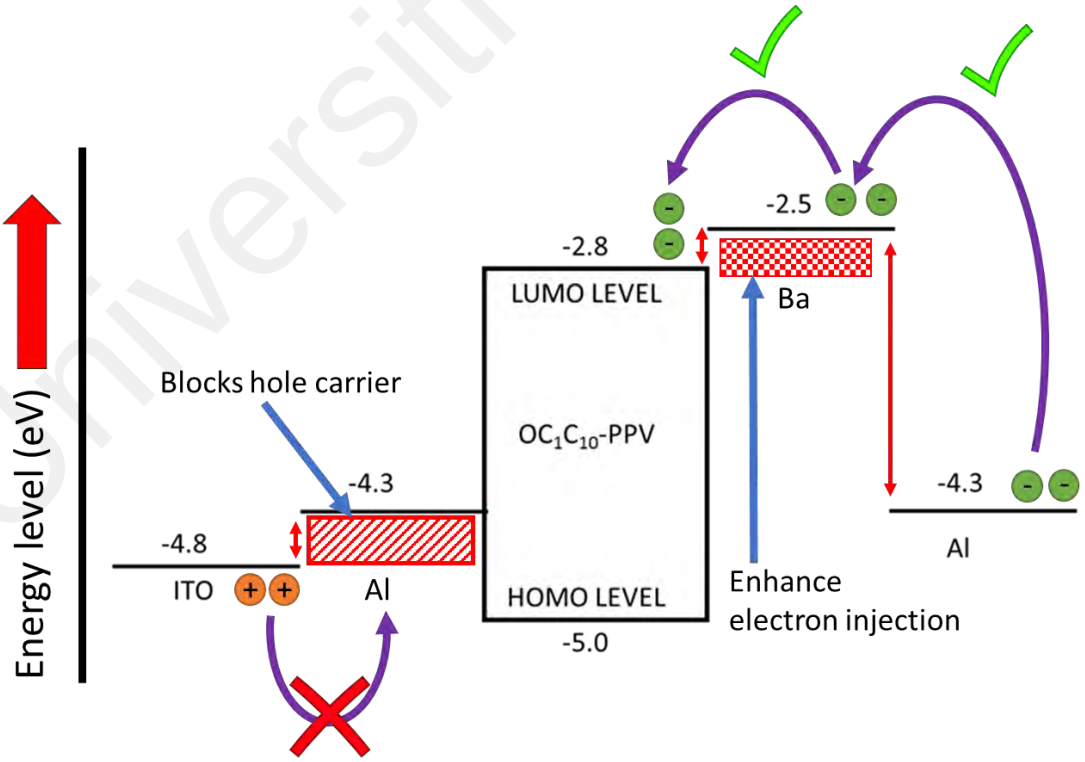

Figure 5.6: Energy band diagram for Electron Only Device (EOD) in OC_1C_{10}-PPV device.

For Figure 5.5, Au has a very low work function and thus has the ability only to allow hole to be injected from the cathode. Al is already established as a good conductor. When it is deposited in between ITO and the OC_1C_{10}-PPV thin-film as shown in Figure 5.6, it is expected that only the electron is favourable and the hole carrier is blocked. The high work function of Barium (Ba) would enhance electron injection from the cathode.

5.2.3 Determination of Trap Density From Current-Voltage of EOD and HOD

The current-voltage plot of HOD and EOD of F8BT material is shown in Figure 5.7, while that of HOD and EOD of OC_1C_{10}-PPV materials are shown in Figure 5.8. Since the data is originated from others people work, Kabra et al. (2010) for F8BT material and Nicolai et al. (2012) for OC_1C_{10}-PPV material, the fabrication method is excluded from this study and the focus is simply just to calculate the trap density from the current-voltage plot.

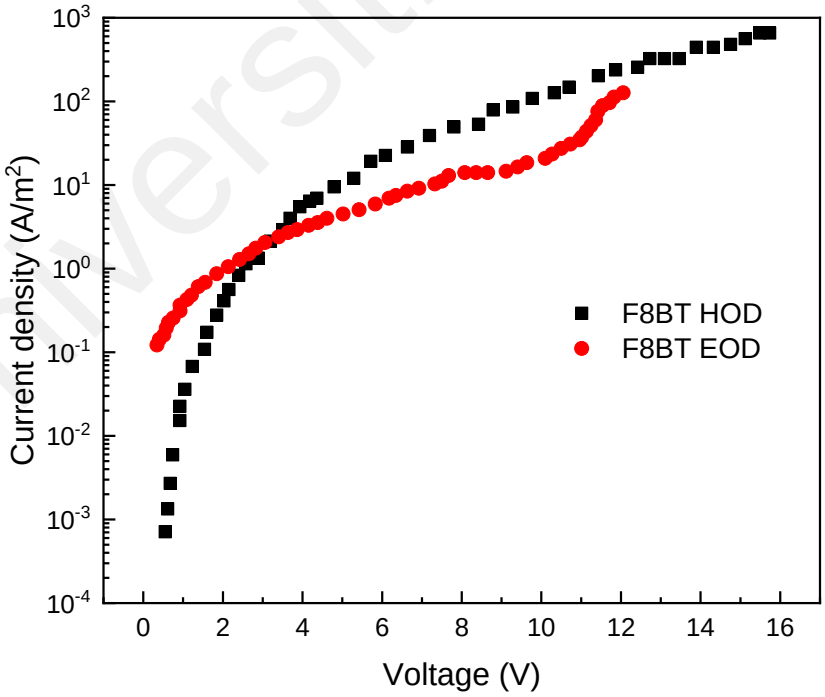

Figure 5.7: Current-voltage relationship for HOD and EOD of F8BT material. (Kabra et al., 2010)

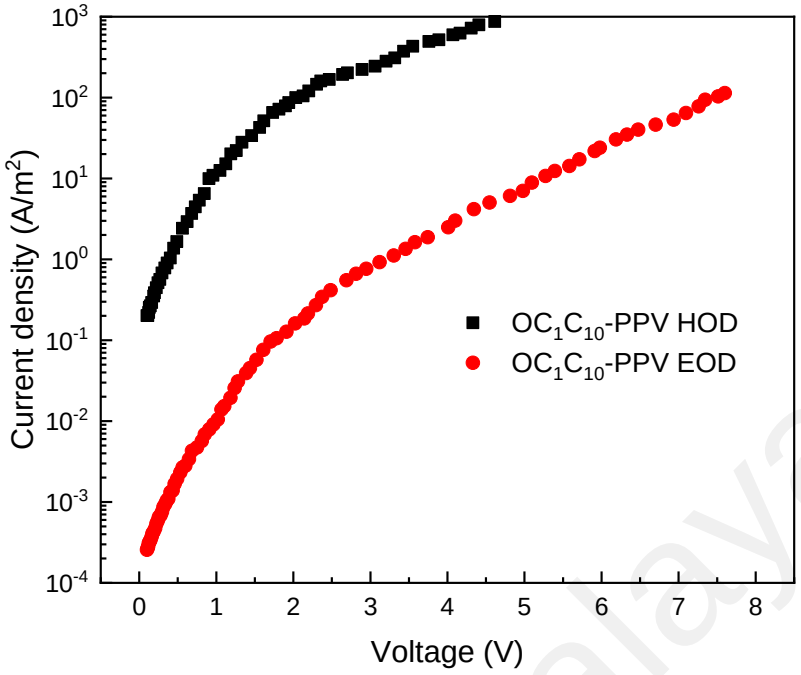

Figure 5.8: Current-voltage characteristic for HOD and EOD of OC_1C_{10}-PPV material. (Nicolai et al., 2012)

From the current-voltage plot, H_t can be calculated by using Equation 3.30 and also values for other parameters stated are given in Table 5.1 for F8BT material, and Table 5.2 for OC_1C_{10}-PPV material. The corresponding values of trap density calculated are then compared with the values reported by others using their respective methods.

Figure 5.9 shows trap density calculated for F8BT-type material as compared with the results obtained by Faria (2011). Figure 5.10 shows trap density calculated for OC_1C_{10}-PPV-type material as compared with the result obtained by Mandoc et al. (2007)

Table 5.1: The parameters used for the estimation of trap density for the F8BT-type material.

	EOD	HOD
N_c, density of state in transport level(m^{-3}) (Burrows & Forrest, 1994)	2.5×10^{36}	2.5×10^{36}
μ, mobility of carrier($m^2V^{-1}s^{-1}$) (Chua et al., 2005)	2×10^{-8}	3×10^{-10}
Temperature(K) (Kabra et al., 2010)	300	300
q, electric charges(C)	1.6×10^{-19}	1.6×10^{-19}
d, thickness of sample(m) (Kabra et al., 2010)	8.7×10^{-7}	8.7×10^{-7}
k, Boltzmann's constant($eV.K^{-1}$)	8.62×10^{-5}	8.62×10^{-5}
T_c, characteristic trap temperature(K) (Chua et al., 2005)	1500	1500
ε_s, permittivity of sample (Park et al. 2011)	3	3
ε_0, permittivity of air	8.85×10^{-12}	8.85×10^{-12}

Table 5.2: The parameters used for the estimation of trap density for the OC_1C_{10}-PPV-type material.

	EOD	HOD
N_c, density of state in transport level(m^{-3}) (Mandoc et .al., 2007)	2.5×10^{24}	2.5×10^{24}
μ, mobility of carrier($m^2V^{-1}s^{-1}$) (Mandoc et al., 2007)	2×10^{-9}	5×10^{-11}
Temperature(K) (Nicolai et al., 2012)	295	295
q, electric charges(C)	1.6×10^{-19}	1.6×10^{-19}
d, thickness of sample(m) (Nicolai et al., 2012)	7.4×10^{-7}	9.8×10^{-8}
k, Boltzmann's constant($eV.K^{-1}$)	8.62×10^{-5}	8.62×10^{-5}
T_c, characteristic trap temperature(K) (Chua et al., 2005)	1500	1500
ε_s, permittivity of sample (Mandoc et al., 2007)	3.9	3.9
ε_0, permittivity of air	8.85×10^{-12}	8.85×10^{-12}

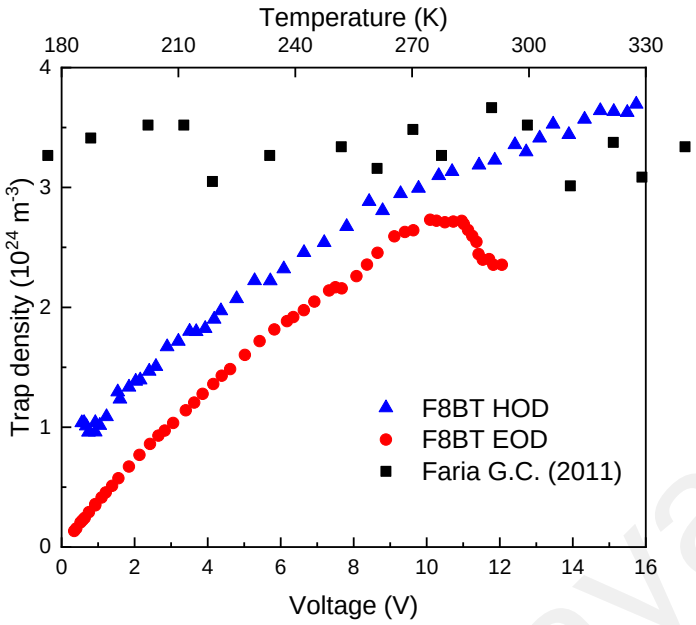

Figure 5.9: Comparison between trap density value calculated using this method and that reported by Faria (2011) for F8BT-type material.

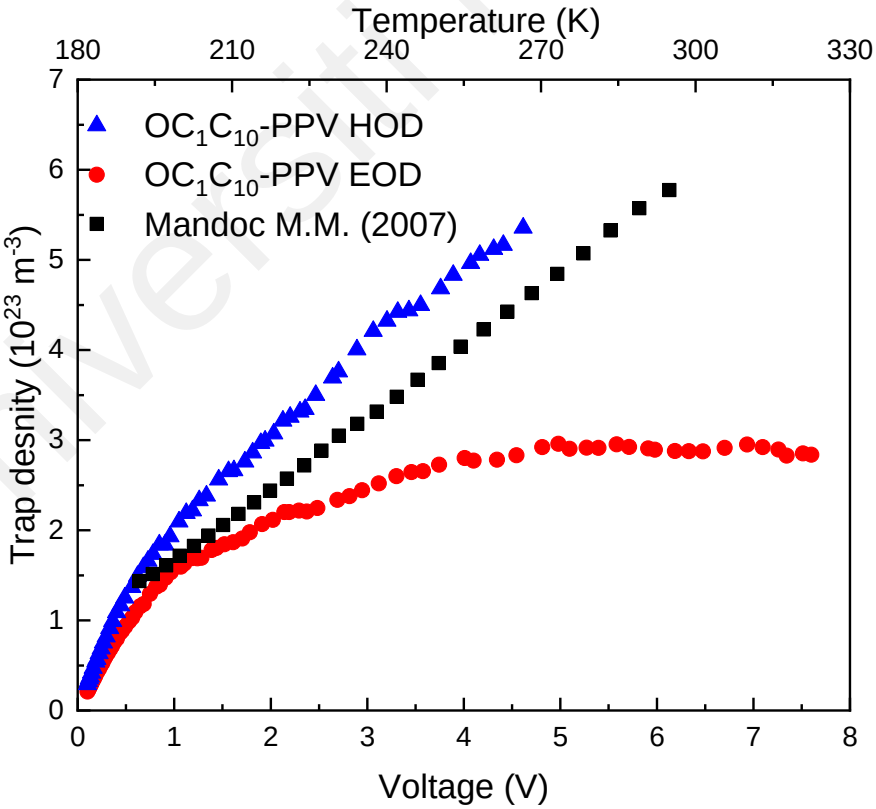

Figure 5.10: Comparison between trap density value calculated using this method and reported by Mandoc et. al., (2007) for OC_1C_{10}-PPV-type material.

5.2.4 Analysis and Discussion of Trap Density of EOD and HOD

From Figure 5.9, trap density for HOD is much higher compared to EOD. In the comparison of device parameter in Table 5.1, it is found that mobility carrier is the main factor contributing to the trap density. Higher trap density is to be expected in HOD as the mobility of the charge carrier of HOD decreases compared to that of EOD which is in agreement with the finding as reported by Horowitz et al. (1995). The same trend can be seen for OC_1C_{10}-PPV -type material, as shown in Figure 5.10.

The trap density of HOD and EOD devices for the two materials depends heavily on the carrier mobility of the device. Even though the trap density values for both types of devices varies from the reported data, they are still comparable to each other (same magnitude) which is 10^{24} m^{-3} for F8BT and $10^{23}m^{-3}$ for OC_1C_{10}-PPV. Figure 5.9 shows that the trap density value obtained by Faria (2011) is almost constant, which suggest that trap density are not temperature-dependent. However, finding by Mandoc et al. (2007) have suggested otherwise, that trap density shows a temperature-dependent relationship. Horowitz et al. (1995) research also report a similar trend to that of Mandoc et al. (2007) that trap density is temperature-dependent.

The finding by Faria (2011) is mainly because of two reasons. First, F8BT devices used by Faria (2011) shows a different current-voltage relationship than the conventional ones. The devices when under a certain value of temperature (i.e. 300 K) have a constant value of current density even when the voltage is varied up to 100V. Second, the method for estimating trap density used by Faria (2011) is known as Trap Fill Limit. This method uses an assumption that trap density should always be a fixed value and the V_{TFL} (trap fill voltage) limit the analysis at the point where the current start increasing. Faria (2011) showed in his thesis, that beyond V_{TFL} value (current density increases), the trap density calculated shows almost linear increment. Thus, leading to a suggestion that trap density

shows a temperature dependency beyond the V_{TFL} . Gaussian disorder models consider the carrier transport in organic thin film as hopping processes with static energetic disorder. This implied that the carrier mobilities has temperature and electric field dependence. Gaussian disorder models required more parameters values or assumption such as zero field mobility, hopping distance of the charge carriers, and the Poole-Frankel factor. Chu et al. (2007) have proved in his work that hole mobility (single carrier device) estimated by SCLC is in excellent agreement with the experimental data measured by time of flight (TOF). Chu et al. (2007) also shown that for thin film thickness less than 300 nm, the difference in values for mobility from the Gaussian Disorder Models are negligible from the values obtained from TOF measurement. The values of mobility used in this work taken from the reference are from TOF measurement and remain valid as shown by Chu et. al where the difference is negligible. The models used for analysis in chapter 5 is enough, fit and comparable with others. One of the main objectives for this thesis, is to provide simple yet reliable method for trap density analysis. Complex models such as Gaussian disorder models would invalidate the objective.

5.3 Conclusion

It is shown that traps density for a single carrier device, EOD and HOD for two types of materials, F8BT and OC_1C_{10}-PPV can be estimated from the current-voltage relationship. Equation 3.30 is used with tables containing values for the parameter of the devices to estimate the trap densities. The values obtained showed a similar trend to those reported by Mandoc et al. (2007) and Faria (2011), and they are also comparable to each other (same order magnitude). The trap density for HOD is much higher than EOD due to the nature of hole carrier having lower mobility than electron carrier. The result from these two types of materials F8BT and OC_1C_{10}-PPV, suggest that the values of trap density for HOD and EOD are temperature-dependent. In Chapter 6, more details on the

trap density analysis would be discussed since it would involve double-carrier devices luminesce due to the formation of excitons in the emissive layer of the devices.

CHAPTER 6: THE EFFECT OF TRAP DENSITY ON LUMINESCENCE OF DOUBLE CARRIER DEVICES

6.1 Introduction

In the previous chapter, Equation 3.30 was used to estimate the trap density values for single-carrier devices, HOD and EOD. The same equation is used again in this chapter to estimate the trap density of a double carrier device (OLED A) that produces luminescence. The values were then compared with others (different method) to show the reliability of this method. Equation 3.16, which calculated the rate of capture process on the localized state, R_n and Equation 3.22, which estimated the de-trapping rate R'_n are then evaluated. The resultant parameters, R_n and R'_n are plotted in the same graph to observe their connection to the luminescence of the device. A simulation is then performed by directly increasing the device trap density. With this simulation, it can be shown that trap density has a strong influence on the R_n and R'_n parameters which have been defined in Chapter 3. A new double carrier device (OLED B) with a hole transport layer (HTL) structure has been fabricated and analyzed in order to confirm the findings obtained from the simulation results. It is expected that OLED B will have higher trap density and thus the device will luminesce at a lower turn-on voltage, as predicted by the simulation results due to the effect of trap density to the parameters R_n and R'_n of the devices.

6.2 Trap Density For Single-layer Organic Devices (OLED A)

A single-layer organic device simply refers to a double carrier device as compared to the single carrier. Since both electron and hole exist simultaneously, the formation of an electron-hole pair is to be expected, and luminescence can be observed. The luminescence is the crucial part of an OLED device where efficiency of the devices can be measured. In Chapter 3, Equation 3.16 and 3.22 values of R_n and R'_n is used to correlate the depth of trap density to the luminescence characteristic of the device. Since several parameters

of the device are involved and required for both equations, OLED A is fabricated in order to extract the much-needed values of the parameters (i.e. the thickness of the device) as indicated in Table 6.1

Chapter 4 has already described all the experimental procedures and characterizations involved for the device fabricated in this chapter. Figure 6.1 shows the energy band diagram for OLED A.

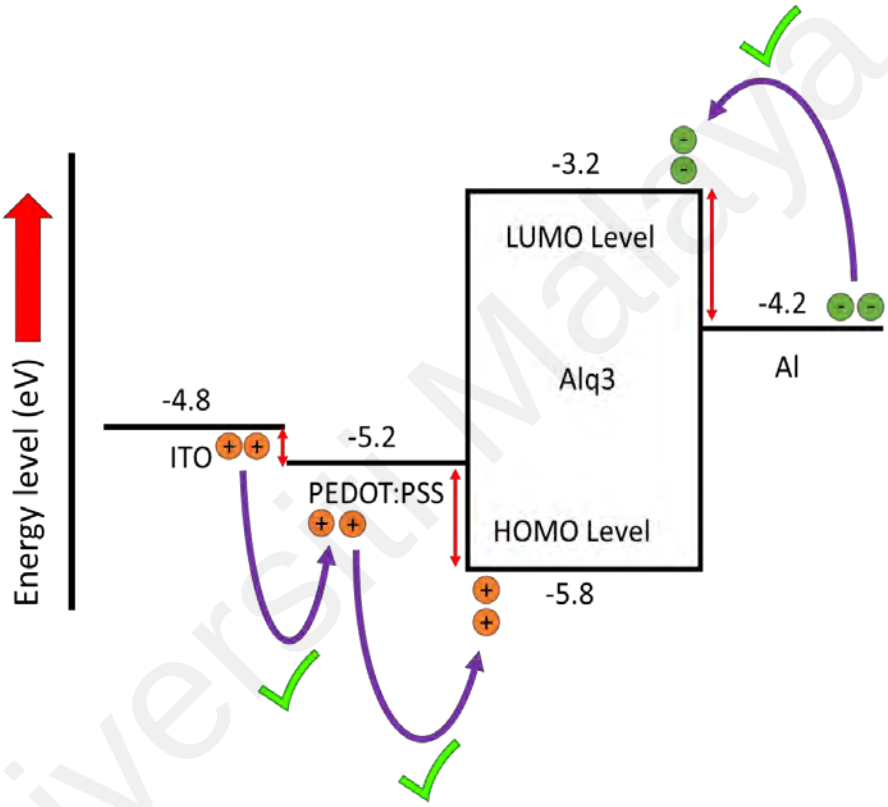

Figure 6.1: Energy band diagram for OLED A.

In Figure 6.1, Alq_3 is the emissive layer where the electron and hole charge carrier will be transported into and recombined. PEDOT:PSS is used as a hole injection layer (HIL) in the device and would facilitate hole injection from the ITO to the Alq_3 emissive layer. Electron charge carrier will be injected from the Al cathode into the Alq_3 emissive layer.

The I-V-L measured from the device characterization is plotted in Figure 6.2. From Figure 6.2, it is observed that the turn-on voltage (device starts emitting light) is 12 V.

The current is at 8.2 mA/cm^2 during the turn-on voltage. The highest luminescence achieved for this device is 191.05 cd/m^2 at 19 V and 48 mA/cm^2.

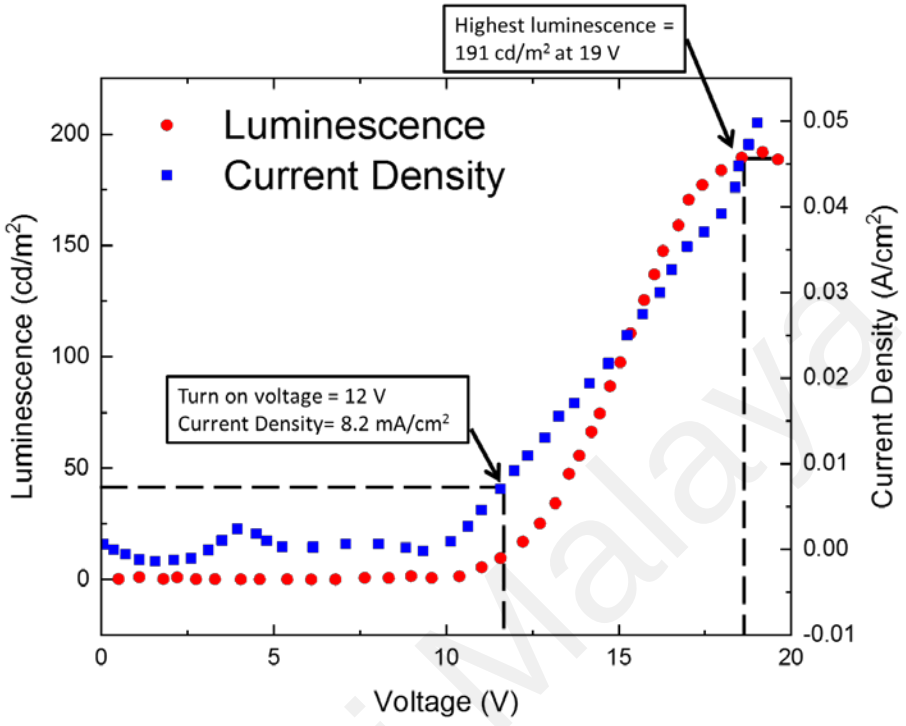

Figure 6.2: J-V-L characteristic of 70 nm OLED A.

Table 6.1: Device parameters for OLED A. (Mężyk et al., 2004)

N_c, density of state in transport level (m^{-3})	2.5 x 10^{36}
μ, mobility of carrier (m^{2}V^{-1}s^{-1})	1 x 10^{-8}
Temperature (K)	300
q, Electric charges (C)	1.6 x 10^{-19}
d, Thickness of sample (m)	7 x 10^{-7}
k, Boltzmann constant (eVK^{-1})	8.62 x 10^{-5}
T_c, characteristic trap temperature (K)	1500
ε_s, permittivity of sample	3
ε_0, permittivity of air	8.85 x 10^{-12}

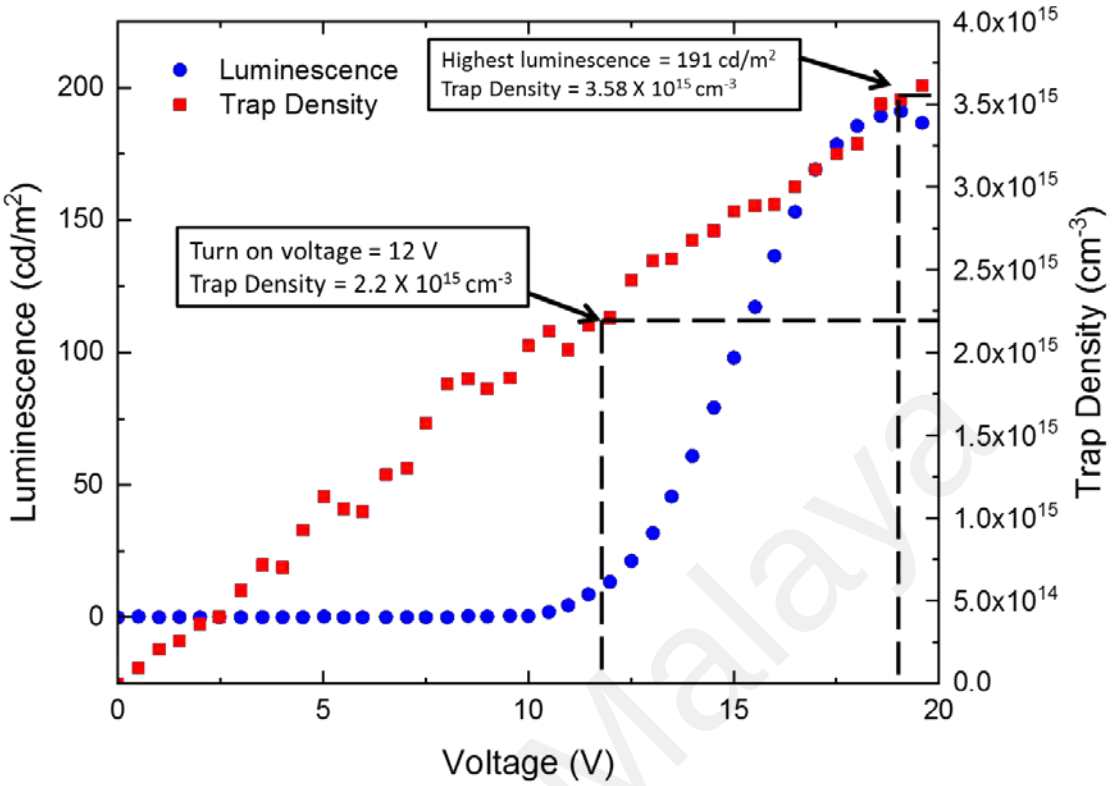

Figure 6.3: Trap density value of OLED A plotted with the luminescence.

The trap density for the Alq_3 device can be estimated using Equation 3.30 with the parameters stated in Table 6.1. The values of trap density are then plotted alongside the luminescence, as shown in Figure 6.3. Tatsuo et al., (1995) published work shown trap density value for Alq_3 device was estimated to be 1.4 X 10^{15} cm^{-3} using the thermal stimulated current (TSC) method. In comparison with the method used in this work, there are two reasons why TSC method would give a slightly difference value. Firstly, TSC uses the assumption that trap density only exists as a single set of carrier traps with a fixed value of trap depth, and the measurement is done in a relatively low-temperature environment, less than 273 K and as low as 173 K. Mandoc et al. (2007) and Horowitz et al. (1995) have already shown that trap density is temperature dependence. Hence, it would explain why the values obtained in this work is higher and in linear form since the

operating temperature is at room temperature (300 K). From Figure 6.3, the result also suggests that the trap density is voltage dependence.

It has been established for the case of a single-carrier device in Chapter 5, that trap density shows temperature dependence. In the case of an OLED device, voltage and temperature are considered parameters that are related to each other. From the literature in Chapter 2, charge carrier injection for an organic semiconductor follows two models, RS (thermionic) injection or F-N tunnelling. For this Alq_3 device, it has been shown through the energy band diagram, that the device is having a relatively low barrier height when the charge carrier is injected at the materials interface. From this, the assumption that RS injection dominates the charge injection in these devices is valid. From Equation 2.2, the current density varies with temperature as:

$$J_{RS} \propto T^2 \tag{6.1}$$

Referring to Figure 6.2, for the device, the current density and the voltage applied showed a linear relationship within a certain voltage range and can be denoted as:

$$J \propto V \tag{6.2}$$

Considering both Equation 6.1 and 6.2, suggesting that trap density is voltage dependence is partially correct, but it should be noted that trap density is also temperature dependence. Since temperature-related studies on OLED device is beyond the scope of this study, only the voltage dependence is investigated in the limit or scope of this research.

From the calculated value of trap density in Figure 6.3, it can be further used to evaluate R_n and R'_n as represented subsequently by Equation 3.16 and Equation 3.22.

Table 6.2 shows all the parameter needed to evaluate both R_n and R'_n. The plot of R_n and R'_n are shown in Figure 6.4 alongside with the luminescence of the device.

Table 6.2: Device parameter and constant used to calculate R_n and R'_n. (Mężyk et. al., 2004)

n, charge carrier concentration (m^{-3})	2.5×10^{36}
n_t, trapped charge carrier (m^{-3})	1×10^{-8}
ς_n, capture cross section (m^2)	1.7×10^{-22}
m_e*, effective mass of electron (1.18 X m_o)	1.7×10^{-30}
d, Thickness of sample (m)	7×10^{-7}
k_B, Boltzmann constant (eVK^{-1})	8.62×10^{-5}
T, operating temperature (K)	300
ΔE_t, trap activation energy (eV)	-0.25
$\hbar$, planck constant (eVs/rad)	6.582×10^{-16}

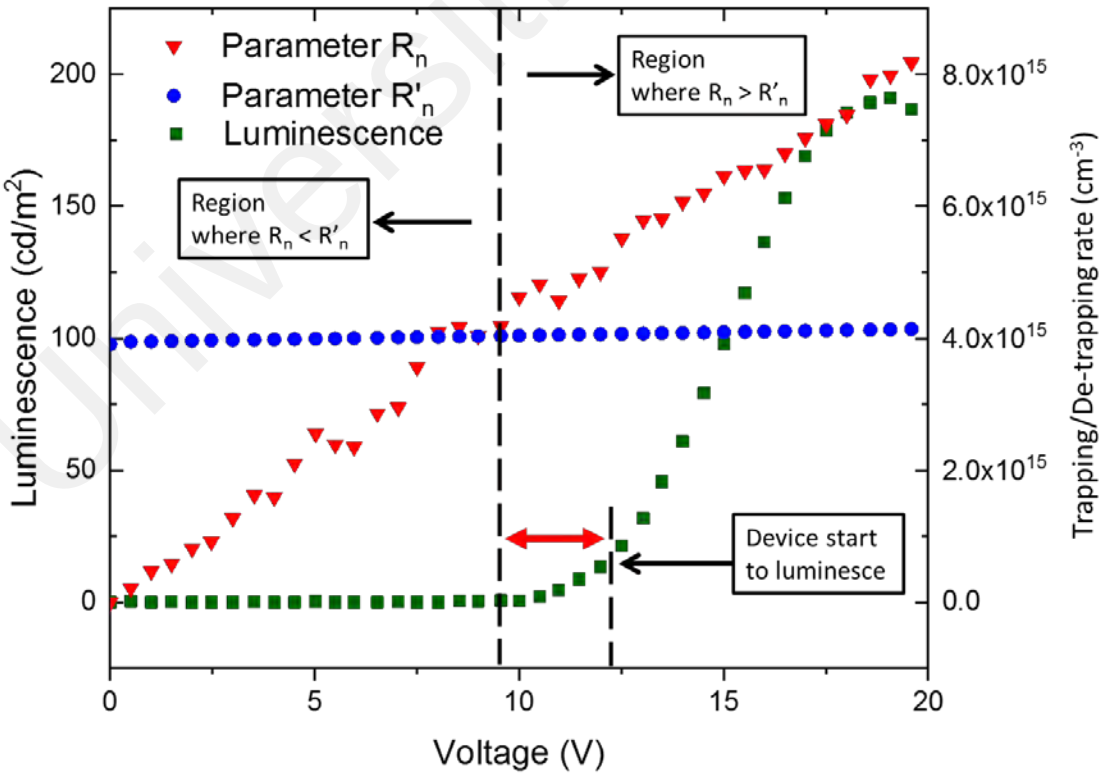

Figure 6.4: Plot R_n and R'_n with the luminescence of OLED A.

From Figure 6.4, it can be seen that the value of R_n, the rate of charge carriers captures (trapping) has increased significantly as the supply voltage increased, while the value of R'_n, the rate of charge carrier release (de-trapping) only have a small increment. When the voltage starts to increase from 0 to 8.5 V, it is observed that the values of R_n are less than R'_n , and when the voltage is further increased from 8.5 to 19 V, values of R_n become greater than R'_n.

It can be established, from Equation 3.16 and 3.22 that when $R'_n > R_n$, the localized state acts as a capture centre (trapping charges) and when $R_n > R'_n$, the localized state acts as a recombination centre. In the case of OLED A, it can be concluded that when R_n is less than R'_n, the emissive layer (localized state) of the device acts as the capture centre and when the values for R_n is greater than R'_n, the emissive layer acts as the recombination centre.

From a theoretical perspective, if the same OLED A device has an increased trap density, R_n and R'_n value also changes and their values are represented in Figure 6.5. If H_t values are increased by two-fold, it can be seen clearly that the region for $R_n < R'_n$ becomes narrower and the region for $R_n > R'_n$ becomes wider. The intersection between R_n and R'_n is shifted to the left. This lead to a hypothesis that the voltage at which the device luminesce can be controlled to a lower value by increasing the trap density of the device.

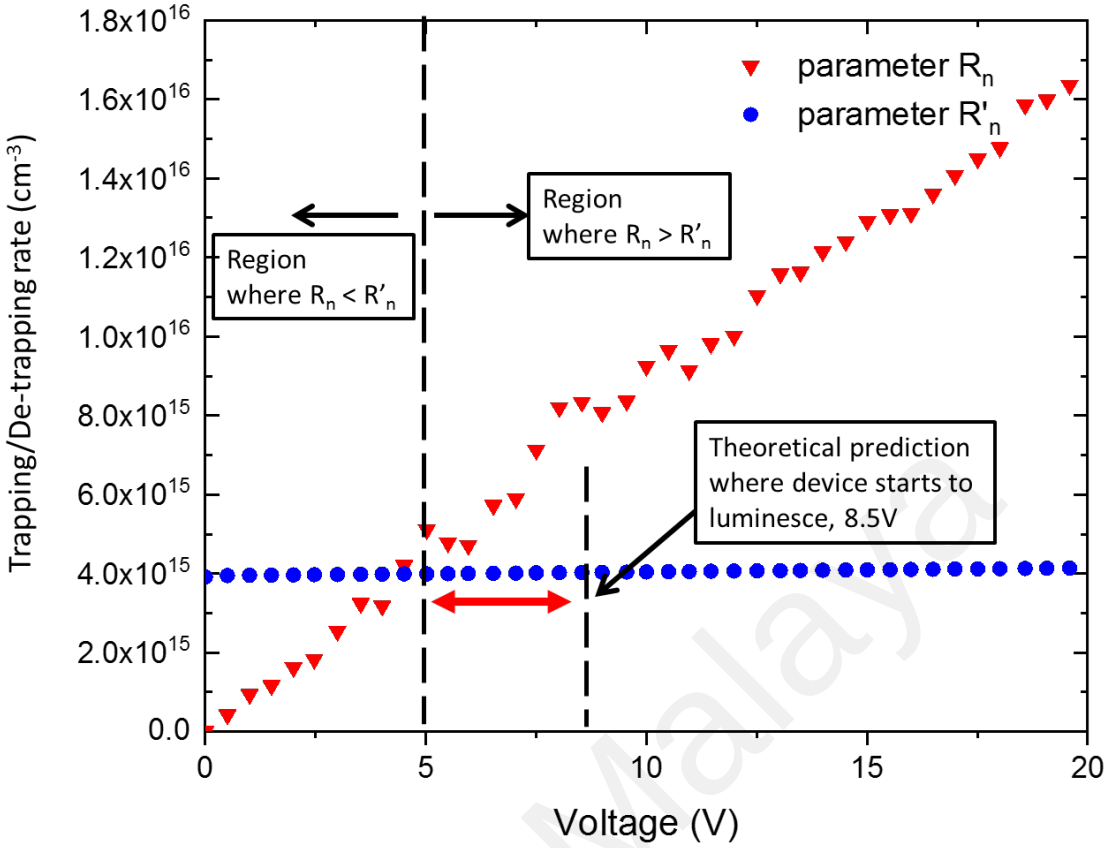

Figure 6.5: Theoretical simulation plot of R_n and R'_n with trap density increased from the original experimental work.

6.3 Trap Density For Single Layer Organic Device with HTL (OLED B)

Daoudi et al., (2016) pointed out in his research finding that a device with HTL has a higher value of trap density than a device without HTL. If a hole transport layer is introduced into the device, the trap density value would increase. To further investigate and verify this theory, a device (OLED B) was fabricated with an added HTL layer of Poly(N,N'-bis-4butylphenyl-N,N'-bisphenyl)benzidine (poly-TPD) with 40 nm thickness to the existing structure of OLED A device. Poly-TPD in the powder form was diluted in chlorobenzene solution with a concentration of 10mg/ml and spin-coated with 2000 rpm for 40 s.

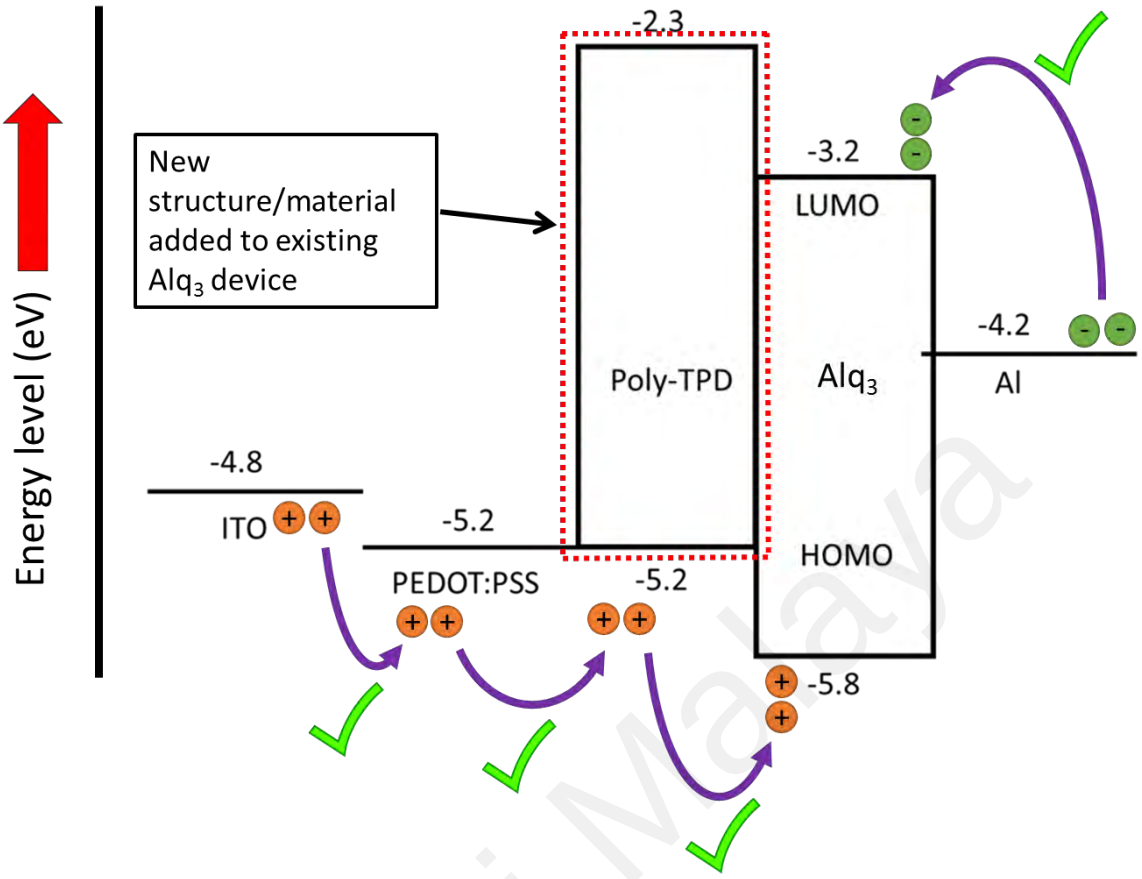

Figure 6.6 : Energy band diagram for OLED B with poly-TPD as the HTL.

Figure 6.6 shows the energy band diagram with the newly added poly-TPD material. With the addition of poly-TPD layer between the PEDOT:PSS and the Alq_3 layer, it acts as a buffer layer for the hole charge carrier transportation from ITO to the Alq_3 emissive layer. Since the value for HOMO level of poly-TPD is the same as the work function of PEDOT:PSS, poly-TPD layer would favour hole carrier instead of an electron, hence poly-TPD is called a HTL.

For the electron charge carrier, no changes occur on the charge transport. Electron injection would flow from the Al cathode to the Alq_3 emissive layer. The J-V-L characteristic of OLED B is shown in Figure 6.7. The device showed an increase in

luminescence peak to 1100 cd/m^2 which was achieved at 16 V compared to that of OLED A where the luminescence peak of 191.05 cd/m^2 was obtained at 19 V.

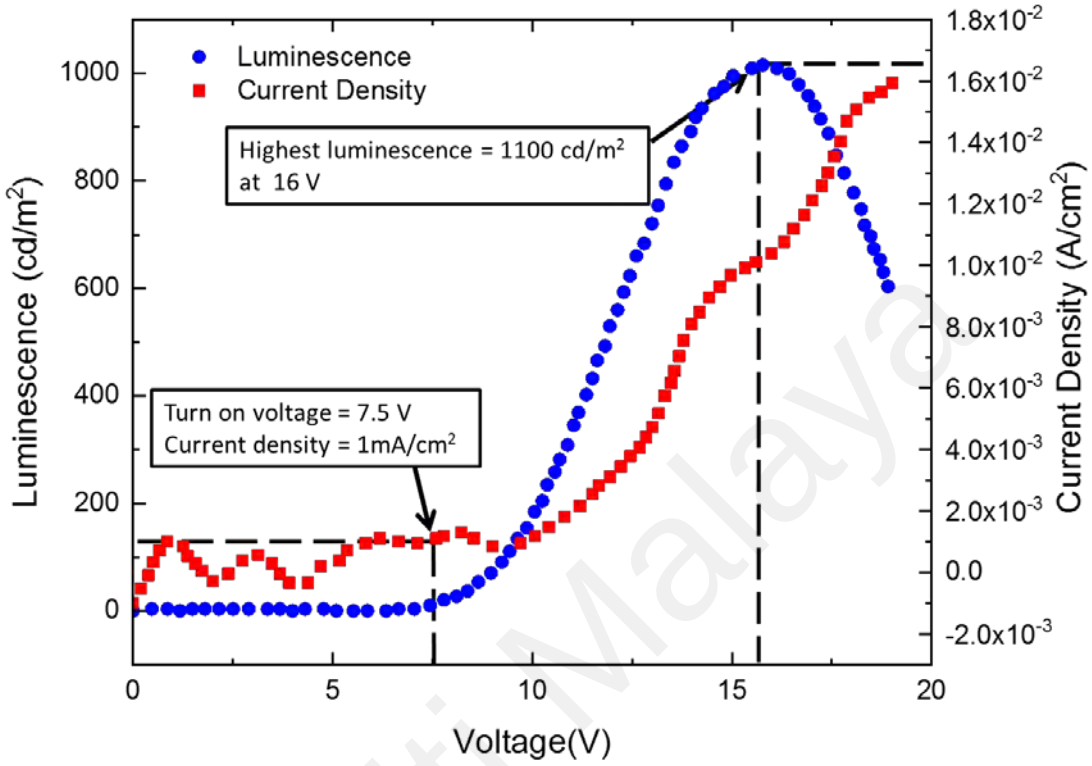

Figure 6.7: J-V-L characteristic of OLED B.

The turn-on voltage is also reduced to 7.5 V with a current density value of 1 mA/cm^2 compared to that of OLED A, with turn-on voltage of 12 V and current density of 8.2 mA/cm^2. These results agree with the experimental work reported by Giebeler et al. (1999). In details, Giebeler et al. (1999) showed that a device structure with a hole transport layer is needed in order to achieve a low operating voltage and a high quantum efficiency. Furthermore, the structure is shown to have efficient hole transfer and limited exciplex formation.

OLED B is then further analyzed using the same analysis as OLED A. By using Equation 3.30 with the help of Table 6.2, the trap density values were calculated, and the results were plotted with luminescence against voltage as shown in Figure 6.8.

Table 6.3: Device parameter for OLED B. (Mężyk et. al., 2004)

N_c, density of state in transport level (m^{-3})	2.5×10^{36}
μ, mobility of carrier ($m^2V^{-1}s^{-1}$)	1×10^{-8}
Temperature (K)	300
q, Electric charges (C)	1.6×10^{-19}
d, Thickness of sample (m)	11×10^{-7}
k, Boltzmann constant (eVK^{-1})	8.62×10^{-5}
T_c, characteristic trap temperature (K)	1500
ε_s, permittivity of sample	3
ε_0, permittivity of air	8.85×10^{-12}

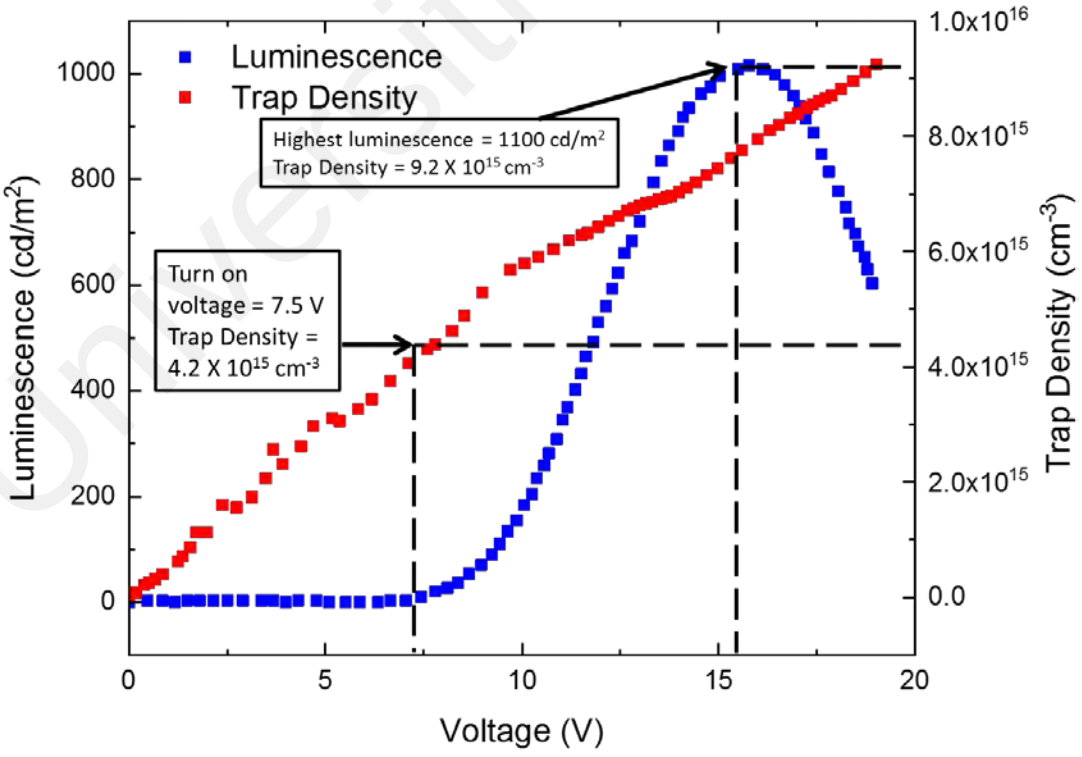

Figure 6.8: Trap density value of OLED B plotted with the luminescence.

From Figure 6.8, it can be proven that with the addition of poly-TPD as the HTL layer, the trap density value for the device has increased by more than two-fold. For OLED B, the trap density value recorded at the turn-on voltage is 4.2 X 10^{15} cm^{-3} compared to 2.2 X 10^{15} cm^{-3} of OLED A. At the highest luminescence achieved, the trap density value is 9.2 X 10^{15} cm^{-3} for OLED B compared to 3.58 X 10^{15} cm^{-3} for OLED A as shown in Figure 6.9. The trap density value doubled at the turn-on voltage and almost tripled at the peak luminesce point when the HTL is introduced in OLED B.The value for R_n and R'_n for OLED B were calculated using the parameter given in Table 6.3. The result was plotted together with luminescence against the voltage applied as shown in Figure 6.9.

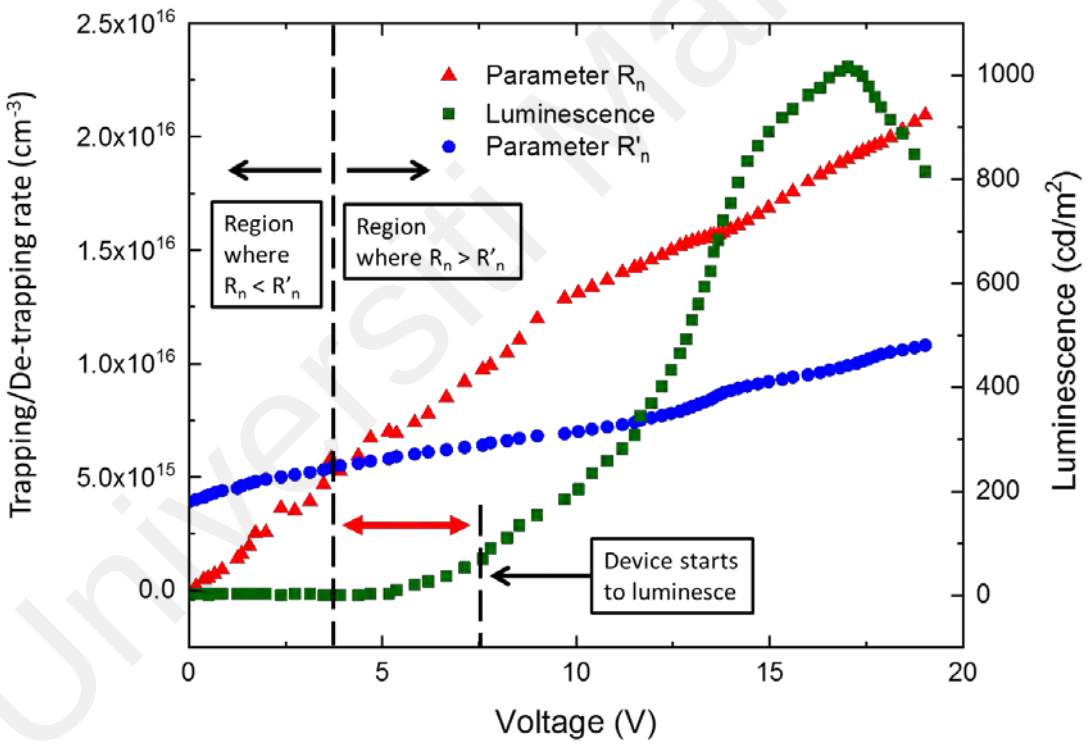

Figure 6.9: Plot R_n and R'_n with luminescence of OLED B.

From Figure 6.9, a similar trend is observed when compared with the results of OLED A, as shown in Figure 6.4. From Figure 6.4 and Figure 6.9 it can be concluded that the device only luminesce in the region where values of the parameter $R_n > R'_n$.

The most interesting part of this research is when the experimental result from Figure 6.9 is compared to the theoretical simulation in Figure 6.5, both figures are shown to have a similar narrow region for $R_n < R'_n$ and a wider region for $R_n > R'_n$. From Figure 6.5, a prediction of turn-on voltage for the device at 8.5 V is made for this particular value of R_n and R'_n. The actual experimental data from Figure 6.9 showed almost similar result as the value for R_n and R'_n are plotted with luminescence.

The actual data from OLED B has shown that the turn-on voltage of the experimental device is slightly lower,at 7.5 V. The small variation from the theoretical plot is caused by trap density value of the actual device is slightly higher than what has been simulated by the theory.

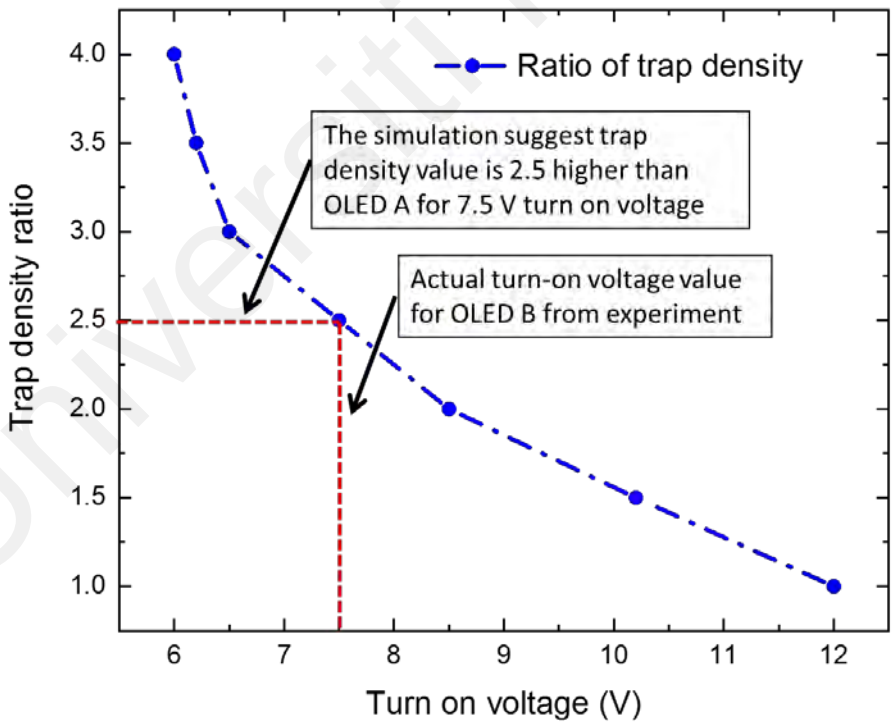

Figure 6.10: Theoretical simulation of trap density variation and the suggested turn-on voltage obtained from the R_n and R'_n plot.

Figure 6.10 shows the simulation plot of the increased trap density ratio of OLED A with the expected turn-on voltage value. When comparing trap density value of OLED B

to that of OLED A at 7.5 V, OLED B has 2.5 times higher trap density value than OLED A. This is consistent with what has been suggested by the theoretical simulation in Figure 6.10.

6.4 Summary

It has already been shown that Equation 3.30 can be used to estimate trap density for double carrier devices (OLED A and OLED B) from the current-voltage characteristic. The values obtained were comparable to those reported by others. The value of trap density can be used to estimate the parameter R_n and R'_n in Equation 3.16 and 3.22, which later were used to analyze the trap density of device. Theoretical simulation has suggested that a higher trap density would lead to an increase in parameter R_n value and the region for $R_n < R'_n$ shrank, while the region $R_n > R'_n$ becomes wider. The theory also suggests that the turn-on voltage would shift to the left, which result in a much lower turn-on voltage for the device. OLED B is fabricated with the addition of poly-TPD layer as HTL to fulfil the condition of higher trap density and validate the theoretical simulation.

The plot of parameter R_n and R'_n of OLED B with higher trap density together with luminescence value of the device has proven that turn-on voltage can be significantly reduced by increasing trap density. The finding agrees with what has been established by the theoretical simulation results reported in this dissertation.

CHAPTER 7: CONCLUSION AND FUTURE WORKS

7.1 Conclusion

This thesis presents an in-depth study of trap density in theory and its effect on the Alq_3 OLED devices. The theoretical study on charge carrier transport is reported in Chapter 3 and the mechanism and nature of trap density were analyzed and discussed in Chapter 5 and Chapter 6. The main findings are concluded in the following paragraphs.

The trap density is not just impurities or defects level that exists inside an organic semiconductor, especially in the emissive materials/part of the device. Shockley-Read Hall theory described trap density as an energy level that exists within the band-gap (HOMO-LUMO level) that able to capture both species of carriers, electron, and holes. Trap density can be described as trapping centre if R_n (trapping rate) < R'_n (de-trapping rate), or as a recombination centre if $R_n > R'_n$. Trap density in OLEDs acts as a catalytic for the recombination process for the electron and hole charge carriers.

Some theoretical study for OLED devices ignored trap density and assumed the electrical profile, current-voltage to follow the SCLC model instead. In Chapter 3 trap density was considered, and the derivation of the current-voltage was shown and discussed. Trap density can be calculated/estimated using Equation 3.30 if all the parameters in the equation are known. In Chapter 5, the trap density calculated showed a temperature-dependence relationship similar to what have been reported by other researchers for EOD and HOD for both F8BT and OC_1C_{10}-PPV materials. It can be concluded that for single-carrier devices, carrier mobilities are the main contribution to the depth of the trap density; hence HOD has higher trap density than EOD due to the nature of hole carrier mobility is lower than electron carrier mobility.

For double-carrier devices (OLED A and OLED B), trap density showed a much more significant effect on the electrical profile (current-voltage-luminescence). Trap density

showed a similar temperature-dependence relationship for OLED A and OLED B, as presented in Chapter 6. R_n, the trapping rate and R'_n, the de-trapping rate is evaluated once the value of trap density is known. Both OLED A and OLED B luminesced only in the region when $R_n > R'_n$. From the simulation, when the trap density was increased, the region $R_n > R'_n$ would be shifted to the left. The simulation suggests that increasing trap density would give a lower turn-on voltage value for a device. Detailed analysis of OLED B J-V-L characteristic and trap density agrees with what has been predicted by the theoretical simulation work where the turn-on voltage of OLED B reduces to a lower value when the trap density is increased in the device.

7.2 Future Works

Based on the research carried out in this work, there are several research questions raised and worthy to study in the future.

(a) In recent years of research in OLED, multi-layer or complex structure built is common, and there are different type of organic layer aside from emissive layer (EML) and hole transport layer (HTL), which are hole blocking layer (HBL), electron transport layer (ETL), hole injection layer (HIL), electron blocking layer (EBL), and electron injection layer (EIL). It would be interesting to see how each layer and/or combination of these layer would affect the trap density value and its impact on the trap density-based analysis.

(b) The emissive materials used in this study is Alq_3, a small molecule organic material. There is already exist different type of organic emissive material such as polymer, quantum dots, blend system, perovskite, and host emissive polymer system. It would be quite a challenge to try using this other type of emissive materials and do the trap density analysis by using the same theoretical simulation technique.

REFERENCES

Adachi, C., Baldo, M. A., Thompson, M. E., & Forrest, S. R. (2001). Nearly 100% internal phosphorescence efficiency in an organic light-emitting device. *Journal of Applied Physics, 90*(10), 5048-5051.

Adachi, C., Tsutsui, T., & Saito, S. (1989). Organic electroluminescent device having a hole conductor as an emitting layer. *Applied Physics Letters, 55*(15), 1489-1491.

Ali, B., Jabar, S., Salih, W., Al Tamimi, R. K., Al Attar, H., & Monkman, A. P. (2009). Synthesis and spectroscopic characterization studies of low molecular weight light emitting PPV segmented copolymers. *Optical Materials, 32*(2), 350-357.

Baldo, M. A., O'brien, D., You, Y., Shoustikov, A., Sibley, S., Thompson, M., & Forrest, S. R. (1998). Highly efficient phosphorescent emission from organic electroluminescent devices. *Nature, 395*(6698), Article#151.

Bell, D. A., & Bell, D. A. (1980). *Electronic devices and circuits*: Reston Publishing Company.

Bhuiyan, A. S., Martinez, A., & Esteve, D. (1988). A new Richardson plot for non-ideal schottky diodes. *Thin Solid Films, 161*, 93-100.

Bonham, J. (1973). SCLC theory for a Gaussian trap distribution. *Australian Journal of Chemistry, 26*(5), 927-939.

Bridge, N. J., & Vincent, D. (1972). Fluorescence and Raman spectra of pure and doped anthracene crystals at 4 K. *Journal of the Chemical Society, Faraday Transactions 2: Molecular and Chemical Physics, 68*, 1522-1535.

Bube, R. H. (1992). *Photoelectronic properties of semiconductors*: Cambridge University Press.

Burroughes, J. H., Bradley, D. D., Brown, A., Marks, R., Mackay, K., Friend, R. H., . . . Holmes, A. (1990). Light-emitting diodes based on conjugated polymers. *Nature, 347*(6293), Article#539.

Burrows, P., & Forrest, S. (1994). Electroluminescence from trap‐limited current transport in vacuum deposited organic light emitting devices. *Applied Physics Letters, 64*(17), 2285-2287.

Chu, T.-Y., & Song, O.-K. (2007). Hole mobility of N,N′ -bis(naphthalen-1-yl)-N,N′ -bis(phenyl) benzidine investigated by using space-charge-limited currents. *Applied Physics Letters, 90*(20), Article#203512.

Chua, L.-L., Zaumseil, J., Chang, J.-F., Ou, E. C. W., Ho, P. K. H., Sirringhaus, H., & Friend, R. H. (2005). General observation of n-type field-effect behaviour in organic semiconductors. *Nature, 434*(7030), 194-199.

Crone, B., Campbell, I., Davids, P., Smith, D., Neef, C., & Ferraris, J. (1999). Device physics of single layer organic light-emitting diodes. *Journal of Applied Physics, 86*(10), 5767-5774.

Daoudi, M., Mendil, N., Berkai, Z., & Belghachi, A. (2016). Study of Trap Density Effect on Current Voltage Characteristics of SubPc and C60 Organic Semiconductors for Photovoltaic Application. In A. Sayigh (Ed.), *Renewable Energy in the Service of Mankind Vol II: Selected Topics from the World Renewable Energy Congress WREC 2014* (pp. 385-391). Cham: Springer International Publishing.

Davids, P. S., Campbell, I. H., & Smith, D. L. (1997). Device model for single carrier organic diodes. *Journal of Applied Physics, 82*(12), 6319-6325.

Donovan, K., & Wilson, E. (1981). Photocarrier creation in one dimension. *Philosophical Magazine B, 44*(1), 31-45.

Faria, G. C. (2011). *Structure and dynamics of poly (9, 9-dioctylfluoren-2, 7-co-benzothiadiazole)(F8BT) and correlations with its electrical properties.* (PhD Dissertation), (São Paulo: University of São Paulo),

Fowler, R. H., & Nordheim, L. (1928). Electron emission in intense electric fields. *Proceedings of the Royal Society of London. Series A, Containing Papers of a Mathematical and Physical Character, 119*(781), 173-181.

Giebeler, C., Antoniadis, H., Bradley, D. D. C., & Shirota, Y. (1999). Influence of the hole transport layer on the performance of organic light-emitting diodes. *Journal of Applied Physics, 85*(1), 608-615.

Gu, G., Burrows, P., Venkatesh, S., Forrest, S., & Thompson, M. (1997). Vacuum-deposited, nonpolymeric flexible organic light-emitting devices. *Optics Letters, 22*(3), 172-174.

Gustafsson, G., Cao, Y., Treacy, G., Klavetter, F., Colaneri, N., & Heeger, A. (1992). Flexible light-emitting diodes made from soluble conducting polymers. *Nature, 357*(6378), Article#477.

Haas, S., Stassen, A. F., Schuck, G., Pernstich, K. P., Gundlach, D. J., Batlogg, B., . . . Kirner, H. J. (2007). High charge-carrier mobility and low trap density in a rubrene derivative. *Physical Review B, 76*(11), 115203.

Habault, D. (1999). Chapter 5 - Analytic Expansions and Approximation Methods. In P. Filippi, D. Habault, J.-P. Lefebvre, & A. Bergassoli (Eds.), *Acoustics* (pp. 159-188). London: Academic Press.

Haering, R. R., & Adams, E. N. (1960). Theory and Application of Thermally Stimulated Currents in Photoconductors. *Physical Review, 117*(2), 451-454.

Hall, R. N. (1952). Electron-hole recombination in germanium. *Physical Review, 87*(2), Article#387.

Higginson, K. A., Zhang, X.-M., & Papadimitrakopoulos, F. (1998). Thermal and morphological effects on the hydrolytic stability of aluminum tris (8-hydroxyquinoline)(Alq3). *Chemistry of Materials, 10*(4), 1017-1020.

Horowitz, G., Hajlaoui, R., & Delannoy, P. (1995). Temperature dependence of the field-effect mobility of sexithiophene. Determination of the density of traps. *Journal de Physique III, 5*(4), 355-371.

Jou, J.-H., Wang, W.-B., Shen, S.-M., Kumar, S., Lai, I. M., Shyue, J.-J., . . . Wu, C.-C. (2011). Highly efficient blue organic light-emitting diode with an oligomeric host having high triplet-energy and high electron mobility. *Journal of Materials Chemistry, 21*(26), 9546-9552.

Jurchescu, O. D., Popinciuc, M., van Wees, B. J., & Palstra, T. (2007). Interface-controlled, high-mobility organic transistors. A*dvanced Materials-Deerfield Beach then Weinheim-, 19*(5), Article#688.

Kabra, D., Lu, L. P., Song, M. H., Snaith, H. J., & Friend, R. H. (2010). Efficient Single‐Layer Polymer Light‐Emitting Diodes. *Advanced Materials, 22*(29), 3194-3198.

Kanno, H., Giebink, N. C., Sun, Y., & Forrest, S. R. (2006). Stacked white organic light-emitting devices based on a combination of fluorescent and phosphorescent emitters. *Applied Physics Letters, 89*(2), Article#023503.

Kepler, R., Beeson, P., Jacobs, S., Anderson, R., Sinclair, M., Valencia, V., & Cahill, P. (1995). Electron and hole mobility in tris (8‐hydroxyquinolinolato‐N1, O8) aluminum. *Applied Physics Letters, 66*(26), 3618-3620.

Kevin, J. Fowler–Nordheim equation. In *Introduction to the Physics of Electron Emission* (pp. 139-148).

Kim, J.-S., Granström, M., Friend, R. H., Johansson, N., Salaneck, W., Daik, R., . . . Cacialli, F. (1998). Indium–tin oxide treatments for single-and double-layer polymeric light-emitting diodes: The relation between the anode physical, chemical, and morphological properties and the device performance. *Journal of Applied Physics, 84*(12), 6859-6870.

Korkin, A., & Rosei, F. (2008). *Nanoelectronics and photonics: from atoms to materials, devices, and architectures* (A. Korkin & F. Rosei Eds. Vol. Nanoelectronics and Photonics). New York: Springer-Verlag New York.

Krellner, C., Haas, S., Goldmann, C., Pernstich, K. P., Gundlach, D. J., & Batlogg, B. (2007). Density of bulk trap states in organic semiconductor crystals: Discrete levels induced by oxygen in rubrene. *Physical Review B, 75*(24), Article#245115.

Kumar, V., Jain, S. C., Kapoor, A. K., Poortmans, J., & Mertens, R. (2003). Trap density in conducting organic semiconductors determined from temperature dependence of J−V characteristics. *Journal of Applied Physics, 94*(2), 1283-1285.

Lampert, M., Rose, A., & Smith, R. (1959). Space-charge-limited currents as a technique for the study of imperfections in pure crystals. *Journal of Physics and Chemistry of Solids, 8*, 464-466.

Lampert, M. A., & Mark, P. (1970). *Current injection in solids*. New York: Academic Press.

Langevin, P. (1903). Recombinaison et mobilites des ions dans les gaz. *Ann. Chim. Phys, 28*(433), Article#122.

Lee, J.-H., Chen, C.-H., Lin, B.-Y., Shih, Y.-C., Lin, K.-F., Wang, L., . . . Lin, C.-F. (2018). Effect of trapped electrons on the transient current density and luminance of organic light-emitting diode. *Journal of Physics D: Applied Physics, 51*(14), Article#144003.

Lee, J.-H., Jeong, J.-H., Suh, C.-H., Kim, Y. K., Park, N. G., & Kim, Y. S. (2006). Numerical analysis of OLED using the hetero electrode. *Current Applied Physics, 6*(4), 654-657.

Lee, T.-W., Noh, T., Choi, B.-K., Kim, M.-S., Shin, D. W., & Kido, J. (2008). High-efficiency stacked white organic light-emitting diodes. *Applied Physics Letters, 92*(4), Article#26.

Lenzlinger, M., & Snow, E. (1969). Fowler‐Nordheim tunneling into thermally grown SiO2. *Journal of Applied Physics, 40*(1), 278-283.

Lenzlinger, M., & Snow, E. H. (1969). Fowler‐Nordheim Tunneling into Thermally Grown SiO2. *Journal of Applied Physics, 40*(1), 278-283.

Li, G. (2011). A novel deep-red-emitting iridium complex with single-peaked narrow emission band: Synthesis, photophysical properties, and electroluminescence performances. *Journal of Luminescence, 131*(2), 184-189.

Li, W., Hagen, J., Jones, R., Heikenfeld, J., & Steckl, A. (2007). Color tunable organic light emitting diodes using Eu complex doping. *Solid-state Electronics, 51*(3), 500-504.

Lü, Z., Deng, Z., Chen, Z., Yin, Y., Xu, D., Xiao, J., & Wang, Y. (2011). The effect of various electrodes on the properties of electroluminescent devices with potassium chloride inside tris (8-hydroxyquinoline) aluminum. *Displays, 32*(3), 113-117.

Lye, R. G., & Dekker, A. (1957). Theory of secondary emission. *Physical Review, 107*(4), Article#977.

MacInnes, D., Druy, M. A., Nigrey, P. J., Nairns, D. P., MacDiarmid, A. G., & Heeger, A. J. (1981). Organic batteries: reversible n-and p-type electrochemical doping of polyacetylene,(CH) x. *Journal of the Chemical Society, Chemical Communications*(7), 317-319.

Mandoc, M. M., de Boer, B., Paasch, G., & Blom, P. W. M. (2007). Trap-limited electron transport in disordered semiconducting polymers. *Physical Review B, 75*(19), Article#193202.

Melpignano, P., Cioarec, C., Clergereaux, R., Gherardi, N., Villeneuve, C., & Datas, L. (2010). E-beam deposited ultra-smooth silver thin film on glass with different nucleation layers: an optimization study for OLED micro-cavity application. *Organic Electronics, 11*(6), 1111-1119.

Mężyk, J., Kalinowski, J., Meinardi, F., & Tubino, R. (2004). Singlet exciton interactions in solid films of Alq3. *Chemical physics letters, 395*(4), 321-326.

Mizuno, Y., Takasu, I., Uchikoga, S., Enomoto, S., Sawabe, T., Amano, A., . . . Adachi, C. (2012). Fluorinated Carbazole Derivatives as Wide-Energy-Gap Host Material for Blue Phosphorescent Organic Light-Emitting Diodes. *The Journal of Physical Chemistry C, 116*(39), 20681-20687.

Neaman, D. A. (1992). *Semiconductor physics and devices*: London:Mcgraw-Hill.

Nicolai, H. T., Kuik, M., Wetzelaer, G. A. H., de Boer, B., Campbell, C., Risko, C., . . . Blom, P. W. M. (2012). Unification of trap-limited electron transport in semiconducting polymers. *Nature Materials, 11*(10), 882-887.

Park, J. S., Lee, B. R., Jeong, E., Lee, H.-J., Lee, J. M., Kim, J.-S., . . . Song, M. H. (2011). High performance polymer light-emitting diodes with N-type metal oxide/conjugated polyelectrolyte hybrid charge transport layers. *Applied Physics Letters, 99*(16), Article#163305.

Pernstich, K. P., Rossner, B., & Batlogg, B. (2008). Field-effect-modulated Seebeck coefficient in organic semiconductors. *Nature Materials, 7*(4), 321-325.

Petr, A., Zhang, F., Peisert, H., Knupfer, M., & Dunsch, L. (2004). Electrochemical adjustment of the work function of a conducting polymer. *Chemical Physics Letters, 385*(1-2), 140-143.

Pope, M., Kallmann, H., & Magnante, P. (1963). Electroluminescence in organic crystals. *The Journal of Chemical Physics, 38*(8), 2042-2043.

Pope, M., & Swenberg, C. E. (1999). *Electronic Processes in Organic Crystals and Polymers*. Oxford: Oxford University Press.

Probst, K. H., & Karl, N. (1975). Energy Levels of Electron and Hole Traps in the Band Gap of Doped Anthracene Crystals. P*hysica Status Solidi (a), 27*(2), 499-508.

Rose, A. (1955). Space-charge-limited currents in solids. *Physical Review, 97*(6), Article#1538.

Ryvkin, S. M. (1964). *Photoelectric Effects in Semiconductors* (1 ed.). New York: Springer US.

Sah, C.-T. (1991). *Fundamentals of solid state electronics*: World Scientific Publishing Company.

Schenk, A. (1992). An improved approach to the Shockley–Read–Hall recombination in inhomogeneous fields of space‐charge regions. *Journal of Applied Physics, 71*(7), 3339-3349.

Shi, W. X., Liu, N., Zhou, Y. M., & Cao, X. A. (2019). Effects of Postannealing on the Characteristics and Reliability of Polyfluorene Organic Light-Emitting Diodes. *IEEE Transactions on Electron Devices, 66*(2), 1057-1062.

Shirakawa, H., Louis, E. J., MacDiarmid, A. G., Chiang, C. K., & Heeger, A. J. (1977). Synthesis of electrically conducting organic polymers: halogen derivatives of polyacetylene,(CH) x. *Journal of the Chemical Society, Chemical Communications*(16), 578-580.

Shockley, W., & Read Jr, W. (1952). Statistics of the recombinations of holes and electrons. *Physical Review, 87*(5), Article#835.

Shuttle, C. G., Hamilton, R., Nelson, J., O'Regan, B. C., & Durrant, J. R. (2010). Measurement of charge‐density dependence of carrier mobility in an organic semiconductor blend. *Advanced Functional Materials, 20*(5), 698-702.

Simmons, J. G. (1965). Richardson-Schottky Effect in Solids. *Physical Review Letters, 15*(25), 967-968.

Sleigh, J., McMahon, D., & Troisi, A. (2009). Effect of the intermolecular thermal motions on the tail of the electronic density of states in polyacene crystals. *Applied Physics A, 95*(1), 147-152.

Sworakowski, J. (1970). Space‐Charge‐Limited Currents in Solids with Nonuniform Spatial Trap Distribution. *Journal of Applied Physics, 41*(1), 292-295.

Sze, S. M. (2008). *Semiconductor devices: physics and technology*: New York:John Wiley & Sons.

Tang, C. W., & VanSlyke, S. A. (1987). Organic electroluminescent diodes. *Applied Physics Letters, 51*(12), 913-915.

Tang, C. W., & VanSlyke, S. A. (1989). Electroluminescent device with improved cathode. In: Google Patents.

Tatsuo, M., Seiya, M., & Teruyoshi, M. (1995). Carrier Transport and Carrier Trap of 8-Hydroxyquinoline Aluminium Thin Films. *Japanese Journal of Applied Physics, 34*(8R), Article#4120.

Thomson, J. J. (1924). XXIX. Recombination of gaseous ions, the chemical combination of gases, and monomolecular reactions. *The London, Edinburgh, and Dublin Philosophical Magazine and Journal of Science, 47*(278), 337-378.

Tsai, M.-J., & Meng, H.-F. (2005). Electron traps in organic light-emitting diodes. *Journal of Applied Physics, 97*(11), Article#114502.

Wang, G.-F., Tao, X.-M., & Wang, R.-X. (2007). *Highly conductive flexible transparent polymeric anode and its application in OLEDs.* Paper presented at the 2007 Proceedings 57th Electronic Components and Technology Conference.

Wantz, G., Hirsch, L., Huby, N., Vignau, L., Silvain, J.-F., Barriére, A., & Parneix, J. (2005). Correlation between the Indium Tin Oxide morphology and the performances of polymer light-emitting diodes. *Thin Solid Films, 485*(1-2), 247-251.

Weiser, K. (1970). Current Injection in Solids. Murray A. Lampert and Peter Mark. Academic Press, New York, 1970. xiv, 354 pp., illus. $18. Electrical Science series. *Science, 170*(3961), 966-967.

Xu, X., Zhu, E., Bian, L., Wang, Z., Wang, J., Zhuo, Z., . . . Tang, W. (2012). Luminescent and photovoltaic properties of poly(9,9-dioctylfluoreneco- bithiophene) in organic electronic devices. *Chinese Science Bulletin, 57*(1001-6538), Article#970.

Xu, Y., Celik, M. A., Thompson, A. L., Cai, H., Yurtsever, M., Odell, B., . . . Brown, J. M. (2009). Tetrameric Iridium Hydride‐Rich Clusters Formed under Hydrogenation Conditions. *Angewandte Chemie International Edition, 48*(3), 582-585.

Zaini, M., Sarjidan, M. M., & Majid, W. A. (2016). Determination of Traps' Density of State in OLEDs from Current–Voltage Analysis. *Chinese Physics Letters, 33*(1), Article#018101.

Zhu, H., Jia, W., Tang, X., Qu, F., Xu, J., Zhao, X., . . . Xiong, Z. (2020). Trap-Enhanced Intersystem Crossing in Tris(8-hydroxyquinoline) Aluminum-Based Organic Light-Emitting Diodes via In Situ Heating. *The Journal of Physical Chemistry C, 124*(5), 3218-3223.

LIST OF PUBLICATIONS AND PAPERS PRESENTED

Published work :

1. **Zaini, M.,** Sarjidan, M. M., & Majid, W. A. (2016). Determination of Traps' Density of State in OLEDs from Current–Voltage Analysis. *Chinese Physics Letters*, *33*(1), Article#018101.

Conference attended:

1. 28th Regional Conference on Solid State Science and Technology (RCSST 2014) 2014, Pahang.
2. 5th International Conference on Solid State Science and Technology (ICSSST 2015) 2015, Kedah.